

# Relating Vegetation Dynamics to Climate Variables in Taiwan Using 1982–2012 NDVI3g Data

Hui Ping Tsai and Ming-Der Yang

**Abstract**—This research aims to improve our understanding of vegetation dynamics and associated climate variables in Taiwan by utilizing mean-variance analysis (MVA), relative directional persistence analysis, and Pearson’s product moment correlation analysis on the Advanced Very High Resolution Radiometer (AVHRR)-derived NDVI3g data from 1982 to 2012. The results indicate a slightly increasing mean-normalized difference vegetation index (NDVI) value with a relatively higher variance during the 1990s and lower variance during the 2000s, which may be explained by the observed fluctuation in precipitation. Additionally, NDVI patterns are identified as increasing in the first half of the year and decreasing in the second half of the year. Spatially, decreasing patterns are observed in all regions except that the northern counties exhibit an increasing NDVI pattern supported by the observed increase in precipitation. Moreover, sunshine duration and temperature are positively correlated with NDVI, whereas precipitation and cloud amount exhibit a negative correlation with NDVI in Taiwan. In the context of global environmental change, this research highlights the utility of applying a combined spatial-temporal approach to remote sensing products. This is an approach with potential applications such as landscape management, conservation practice, and water resource management for policy makers and stakeholders in and beyond Taiwan.

**Index Terms**—Advanced Very High Resolution Radiometer (AVHRR), climate, correlation, mean-variance analysis (MVA), normalized difference vegetation index (NDVI), persistence, precipitation, remote sensing, Taiwan, vegetation.

## I. INTRODUCTION

**M**ONITORING vegetation change over regional scales using earth observing satellite data has greatly improved our understanding of vegetation dynamics [1]–[5]. As a way to understand these vegetation changes, normalized difference vegetation index (NDVI) time series data acquired by sensors aboard satellites have been widely used since it provides an efficient, repeatable, and consistent measurement to reflect the response of the earth’s ecosystem to interannual and intraannual dynamics of biotic and abiotic drivers [6]–[10].

The NDVI derived from the Advanced Very High Resolution Radiometer (AVHRR) onboard the National Oceanic and Atmospheric Administration’s (NOAA) satellite series has been considered as the longest temporal coverage and the best

data set available for long-term analysis of vegetation dynamics [11], [12]. NDVI is calculated as near-infrared spectrum (NIR)-RED/NIR+RED to express the contrast between the two spectra because the chlorophyll of vegetation absorbs strongly in the red light spectrum (RED), whereas the cell structure of the leaves reflects and scatters light in the high near-infrared spectrum (NIR). NDVI has been closely linked with the fraction of green vegetation, serving as a measurement of vegetation abundance that has been applied to a number of vegetation indicators and characteristics such as climate variability [13]–[22], net primary productivity [23]–[28], land cover classifications [29]–[33], vegetation phenology [34]–[42], drought detection [43]–[48], and land degradation [49]–[54].

Climate variability is one of the major drivers controlling interannual and intraannual vegetation variations. The relationship between NDVI and climate variables has been extensively studied worldwide [55]–[66]. Studies have suggested that precipitation and temperature are two major climate factors that are linked closely to vegetation growth through the process of photosynthesis [67]–[71]. Other factors such as land cover and land use change (LULCC), sunshine duration, cloud amount, soil moisture, and evapotranspiration all contribute to vegetation variation in diverse degrees [72]–[74]. Considering the location, unique topography, and ecological characteristics of Taiwan, understanding the relationship between NDVI and relevant climate factors is critical to managing landscapes for the joint benefit of human and natural systems. Several studies have used vegetation indices to study the vegetation dynamics in Taiwan. Chang *et al.* [75] related vegetation dynamics to temperature and precipitation using Moderate Resolution Imaging Spectroradiometer (MODIS) Enhanced Vegetation Index (EVI) data from 2000 to 2012 and found that the relationships between EVI and temperature and between EVI and precipitation are temporal scale dependent and vegetation/land-use-type dependent. Another study applied principal component analysis (PCA) to MODIS photosynthetically active vegetation cover (PV) data to investigate interannual vegetation dynamics in Taiwan from 2001 to 2011 [76]. Those findings reveal that the sensitivity of Taiwan’s ecosystems may not only be controlled by regional climate and human activities but may also be susceptible to large-scale climate anomalies such as the El Niño Southern Oscillation (ENSO) [77], [78].

Additionally, many scholars have applied NDVI as a measurement to assess short-term landscape change detection in Taiwan, such as postdisaster evaluation [79]–[87], wetland analysis [88], forest area evaluation [89], [90], and crop evaluation [14], while others have applied NDVI to ecological research [91]–[93], land cover classification [76], and modeling

Manuscript received August 12, 2015; revised December 07, 2015; accepted December 15, 2015. Date of publication January 25, 2016; date of current version March 11, 2016. This work was supported by the Ministry of Science and Technology of Taiwan under Project MOST 103-2625-M-005-008-MY2. (Corresponding author: Ming-Der Yang.)

The authors are with the Department of Civil Engineering, National Chung Hsing University, Taichung 402, Taiwan (e-mail: mdyang@nchu.edu.tw).

Color versions of one or more of the figures in this paper are available online at <http://ieeexplore.ieee.org>.

Digital Object Identifier 10.1109/JSTARS.2015.2511742

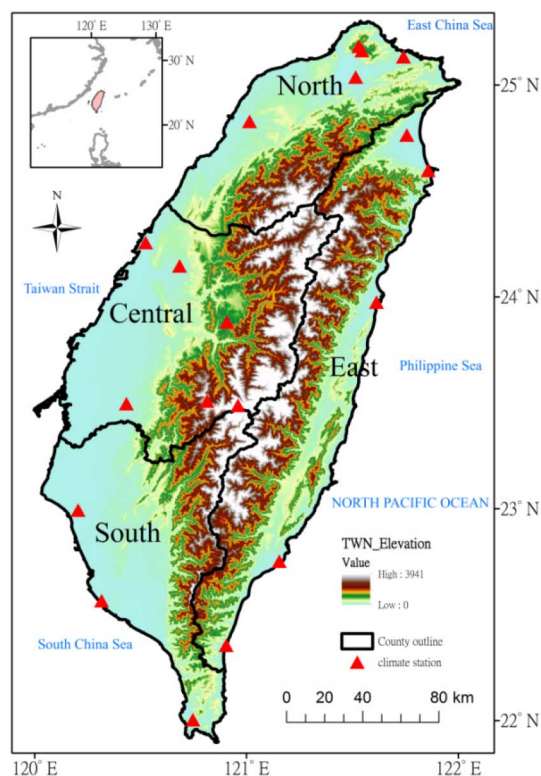


Fig. 1. Study area.

[94]. Understanding vegetation dynamics is critically important for explaining both abiotic–biotic interactions and providing scientific assessments that can aid further environmental studies, modeling, and predictions. However, an integrated analysis of long-term vegetation dynamics in Taiwan is missing and its relationship with climate factors remains unexplored.

To fill in this gap, this study applied the mean-variance analysis (MVA), relative directional persistence metric, and Pearson’s product moment correlation analysis to investigate more than three decades of vegetation dynamics (via AVHRR NDVI3g data) and its relationship with climate variables in Taiwan from 1982 to 2012. In this study, a comprehensive island-wide overview of NDVI patterns is assessed so as to answer three specific research questions: 1) what is the overall long-term NDVI pattern in Taiwan between 1982 and 2012? 2) how is the spatial pattern of monthly NDVI varied in Taiwan? and 3) what is the relationship between NDVI and climate variables, such as temperature and precipitation?

## II. METHODOLOGY

### A. Study Area

Taiwan (22°–25°N, 120°–122°E, Fig. 1) is an island located at the western edge of the Pacific Ocean between Japan and the Philippines and has a total land area of approximately 36 000 km<sup>2</sup>. With a population that increased from 20.4 million in 1990 to 23.3 million people in 2013, Taiwan is experiencing growing pressure from its dense population (645 people/km<sup>2</sup>) [95].

The annual precipitation in Taiwan is approximately 2500 mm, and the mean temperature is approximately 22 °C–25 °C [96]. Taiwan’s climate variations are primarily affected by the East Asian monsoon [97], [98] and further complicated by the mountainous topography and land-sea distribution [99], [100]. The Central Mountain Range (CMR) stretches from the north to the south with the highest point at Yu Mountain (3952 m); this mountain range divides the island into the west and east coasts. In general, the climate in Taiwan is a marine subtropical to tropical climate, which is considered to be humid with moderate to high temperatures all year long; however, large spatial variations exist throughout the course of the year [97], [101], [102].

In general, Taiwan’s climate can be separated into the cold season (September–April) and the warm season (May–August) [97]. During the cold season, precipitation in Taiwan is influenced by the northeasterly monsoon, while the southwesterly monsoon affects Taiwan during the warm season [103], [104]. Additionally, a variety of transient subsynoptic disturbances such as springtime cold fronts, Mei-Yu fronts, typhoons in the summer months, and cold fronts in the fall all contribute to the precipitation mechanism in Taiwan [97], [101], [104]. In addition to the prevailing monsoon flow, local rain showers related to terrain or local winds also play an important role in generating precipitation. According to Taiwan’s diverse precipitation mechanism, Wang *et al.* [105] categorized the rainfall regimes in Taiwan into five categories: 1) winter (December–February); 2) the spring transition (March and April); 3) the Mei-Yu season (mid-May to mid-June); 4) the typhoon season (mid-July to August); and 5) the autumn rainfall regime (September–November). Based on previous studies and for convenience in analysis, this study describes December–February as the winter season, March–May as the spring season, June–August as the summer season, and September–November as the fall season.

Furthermore, Taiwan’s precipitation regimes exhibit a high level of spatial heterogeneity resulting from its diverse topography and rainfall mechanism. For the northern part of island, the spring rain (February–April) plays an important role [97]. The northeasterly monsoon and tropical cyclone bring heavy rains for the eastern part of the island from September to November. The main rainy season for the central and southern parts of the island occurs during the warm seasons with the Mei-Yu fronts (May–June), summer afternoon convective activity, and tropical cyclones, while the typical dry season starts in October [103].

### B. NDVI Data

The third generation of the AVHRR NDVI3g dataset developed by Global Inventory Modeling and Mapping Studies (GIMMS) group was utilized in this research [106]. The AVHRR NDVI3g dataset has a temporal resolution of 15 days and a spatial resolution of 1/12 degree (approximately 8 km) and spans the period from July 1981 to December 2012. The AVHRR NDVI3g dataset is generated from a series of AVHRR sensors in the framework of the GIMMS project at NASA’s Goddard Space Flight Center. NDVI values are calibrated using Vermote and Kaufman’s atmospheric Rayleigh scattering over oceans methods. Volcanic stratospheric aerosol

periods (1982–1984 and 1991–1994) have been established and subjected to atmospheric corrections [107]. The empirical decomposition (EMD) reconstruction methods were applied to correct the satellite orbital drift effect [108]. Additional improved cloud masking and SeaWiFS NDVI data were used to calibrate AVHRR NDVI3g data using Bayesian methods [109] in order to minimize factors unrelated to changes in vegetation greenness. The 15-day NDVI3g data were aggregated from the daily data using maximum value compositing method [109], [110] to reduce cloud and aerosol contamination [111]. The AVHRR NDVI3g dataset is the currently longest available NDVI dataset providing vegetation cover worldwide, which offers a unique opportunity for long-term vegetation pattern analysis. For this study, the image with higher value in each month was obtained from January 1982 to December 2012, and Taiwan’s land area was extracted for further analysis.

### C. Climate Variables

Precipitation and temperature data were derived from the Taiwan Climate Change Projection and Information Platform (TCCIP) for the study period of 1982–2012 at a monthly time scale with a spatial resolution of  $5 \times 5 \text{ km}^2$ . The TCCIP datasets were generated using the inverse distance weighted interpolation and weighted average methods suggested in [112].

The monthly cloud amount and sunshine duration data (in hours) were obtained from the Central Weather Bureau of Taiwan from 19 weather stations across the landscape for the study period 1982–2012. These 19 weather stations were selected based on the best available environmental data covering the study period. Of the 19 weather stations, there are five, six, three, and five stations located in the northern, central, southern, and eastern counties, respectively (Fig. 1). These 19 weather stations are considered as representatives for the four major regions of Taiwan and can reflect the characteristics of NDVI in Taiwan.

### D. Mean-Variance Analysis

The MVA was developed to characterize an overall spatial and temporal patterns of imagery [113] rather than local patterns that are resulted from clustering or morphological segmentation [114], [115]. Later, many scholars adapted the method to delineate seasonal and interannual responses of vegetation to climate and disturbances [116]–[119]. The MVA depicts dynamic systems graphically as a time-evolving process by plotting the mean of the vegetation index (VI) response versus its variance on a portrait.

A hypothetical relationship between mean-variance and vegetation status is shown in Fig. 2 [117]. The mean of VI can be interpreted as the overall amount of vegetation within the landscape ( $X$ -axis), and the variance can be interpreted as the degree of landscape heterogeneity ( $Y$ -axis). Additionally, the grand mean reference lines from the mean and variance of VI ( $X$ - and  $Y$ -axes) classify the portrait into four quadrants, where each quadrant reveals divergent degrees of spatial heterogeneity (variance) and vegetation status (mean). Generally, Quadrant 1 (low mean and variance) symbolizes the most

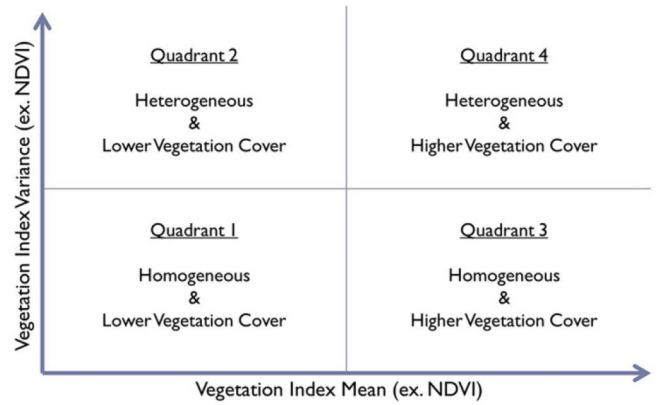


Fig. 2. Hypothetical relationship between the mean variance of a vegetation and landscape status (adapted from [117]). The  $X$ -axis represents the mean of a specific VI, while the  $Y$ -axis represents the spatial variance. Each quadrant indicates the status of a landscape.

degraded landscape, with homogeneously lower vegetation cover. Quadrant 2 (low mean and high variance) suggests a high proportion of the landscape tending toward bare ground, which is thus prone to disturbance. Quadrant 3 (high mean and low variance) implies greater homogeneous vegetation cover, and Quadrant 4 (high mean and variance) indicates that the landscape possesses both higher vegetation cover and a higher spatial variability. Interpretations of the “ideal” quadrant for a landscape, however, must be performed with caution by considering the dominant land cover.

MVA manifests the motion or trajectory of vegetation status through time. In this study, NDVI patterns were examined on two temporal scales: annual (averaged value of NDVI from January to December) and seasonal for fall/winter (October–March) and spring/summer (April–September).

### E. Relative Directional Persistence Metric

The relative directional persistence metric  $R$  is one of three persistence metrics recently developed in [120], and it has been applied by several scholars for vegetation research [68], [121]. The metric  $R$  is designed to capture the directional increase/decrease change of NDVI. Essentially, the values of NDVI are assumed to be normally distributed and serially independent under the condition of no disturbances such as LULCC and climate variability. The assumption of  $R$  was carefully validated and verified by a simple Monte Carlo simulation (simulated  $n = 10\,000$ ) and extensive empirical observations. Detailed validation and verification process can be found in [120, pp. 4478–4483]. Based on the assumption, the statistical significance levels of  $R$  can be set in order to highlight areas that are marked by unexpected changes.

$R$  makes comparisons relative to the observation in the preceding year. For instance, an observation from June 1983 is compared to one from June 1982 and thus reveals sequential cumulative directional change

$$R_j = \sum_{i=2}^n t_{i,j} \quad (1)$$

$$V_{i,j} < V_{i+1,j} : t_{i,j} = +1 \quad (2)$$

$$V_{i,j} > V_{i+1,j} : t_{i,j} = -1 \quad (3)$$

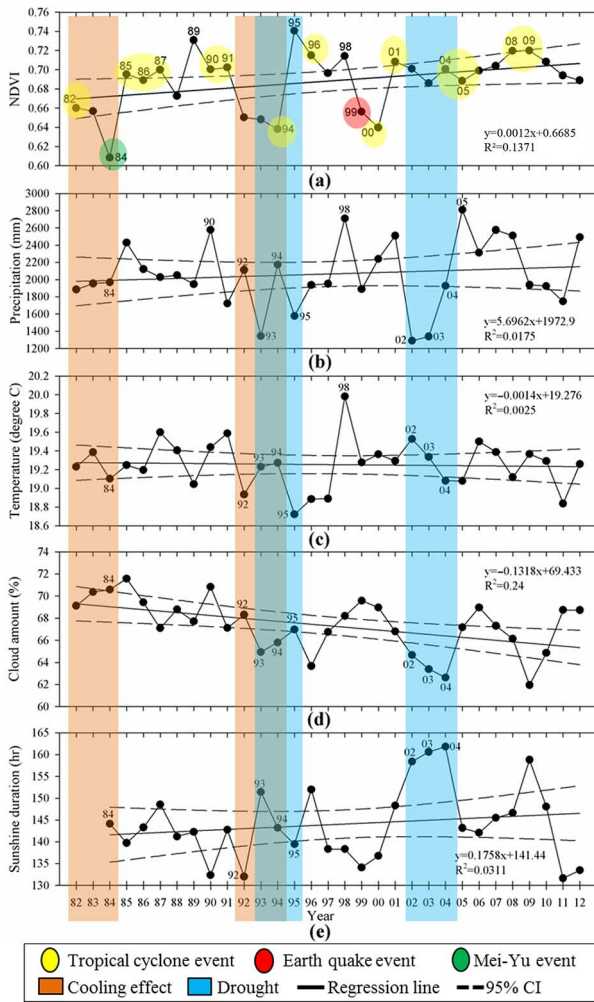


Fig. 3. NDVI and climate variables are shown for the period from 1982 to 2012 (sunshine duration data period from 1984 to 2012). The linear regression line (solid line) with its 95% confidence intervals (dashed line) is shown with regression equations and  $R$  squared. (a) Annual mean NDVI. (b) Annual precipitation (mm). (c) Annual mean temperature. (d) Annual mean cloud amount (%). (e) Annual mean sunshine duration (h).

where  $V_{i,j}$  is the monthly value of NDVI, in year  $i$ , month  $j$ . A value of  $+1$  is assigned if a pixel records a value of NDVI greater than that in the preceding year, and  $-1$  is assigned if it is less. After summing all the assigned new values, the resulting  $R$  reflects the sequential cumulative relative directional change of NDVI.

### III. RESULTS

#### A. Interannual Variations in NDVI and Climate Variables

The variations of annual mean NDVI of Taiwan and corresponding climate variables, including precipitation, temperature, cloud amount, and sunshine duration, are shown in Fig. 3. Overall, NDVI, precipitation, and sunshine duration increase slightly from 1982 to 2012, while the temperature and cloud amount show a tendency to decrease; however, neither NDVI nor any climate variables reveal a statistically linear significant trend (0.05 level) (Fig. 3).

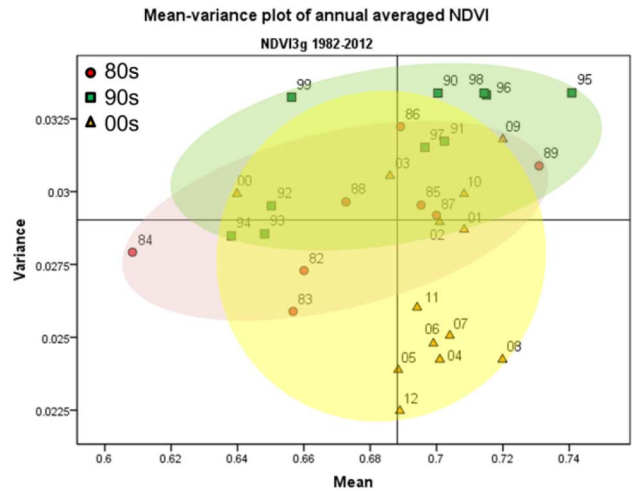


Fig. 4. Mean and variance for annual averaged NDVI throughout Taiwan.

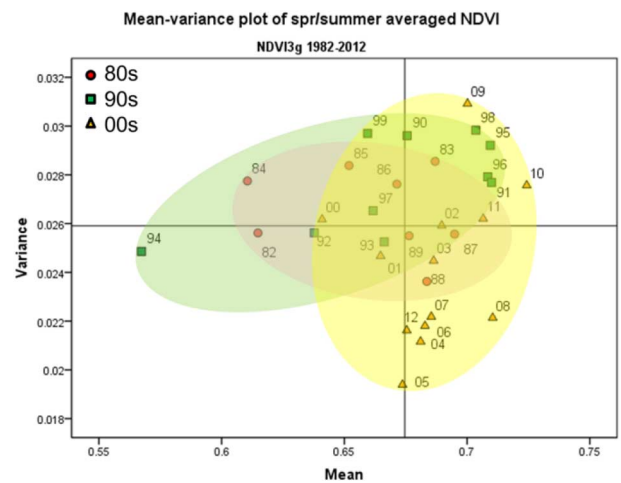


Fig. 5. Mean and variance for spring/summer (March–August) averaged NDVI.

#### B. Mean-Variance Analysis

The annual NDVI shows a slight increase from the 1980s to 2000s, while the spatial variance peaks during the 1990s (Fig. 4). The low mean and low variance of the NDVI value in the early 1980s indicates a relatively homogeneous landscape with lower amount of vegetation cover. The increase in both the mean and spatial variance values after 1985, however, represents an increasing spatial heterogeneity and higher amount of vegetation. The values revert to a lower mean and variance during the early 1990s (1992–1994), although a noticeable rise in both mean and variance after 1994 reflects significant growth rates and high variability across the landscape. The dominant pattern of vegetation cover in the 1990s, however, is one of the relatively high spatial variance with a mean value increasing in the later years. High mean values are maintained in the 2000s (NDVI mean=0.69), while the spatial variance is generally lower than the long-term average. Similar patterns can be found in both spring/summer and fall/winter data (Figs. 5 and 6).

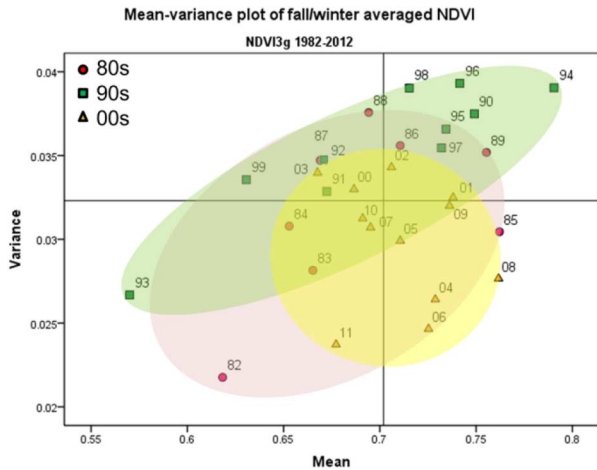


Fig. 6. Mean and variance for fall/winter (September–February) averaged NDVI.

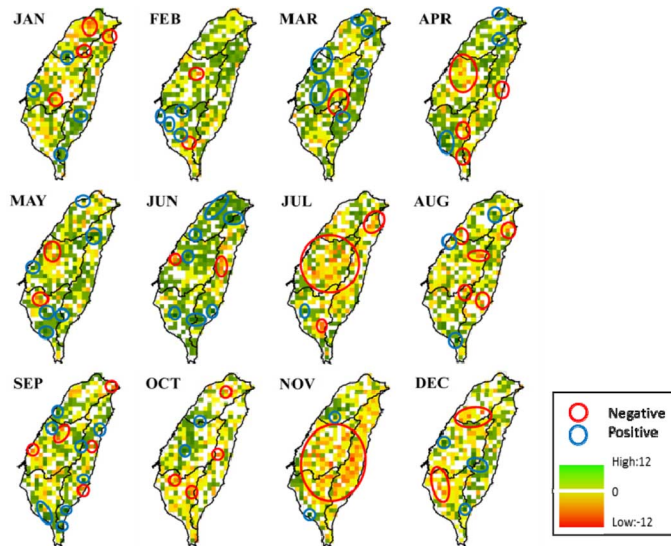


Fig. 7. Scores of relative directional persistence metric  $R$  for January–December, 1982–2012. Positive values are shown in green gradient, negative values are shown in red gradient, and the zero value is shown in white. Statistically significant (0.05 level) pixels are circled in blue (positive) and red (negative).

### C. Relative Directional Persistence Metric

The result of the relative directional persistence metric in Fig. 7 shows pixels with positive scores ( $R > 0$ ), negative scores ( $R < 0$ ), and zero score ( $R = 0$ ). Hereafter, pixels with positive scores will be assumed to have an increasing pattern of NDVI during the study period from 1982 to 2012. Likewise, pixels with negative scores will be considered to have a decreasing pattern of NDVI. Pixels with zero scores will be presumed to have no discernible change in NDVI over the study era. However, it is necessary for the limitations of  $R$  to be mentioned and interpreted with caution. Based on (1)–(3),  $R$  can capture the direction of change; however,  $R$  is not sensitive to the magnitude of change. For instance, the differences between large and small magnitudes of positive change would not reflect on the value of  $R$ , but instead yield the same value. As such, the results of  $R$  values need to be interpreted with caution.

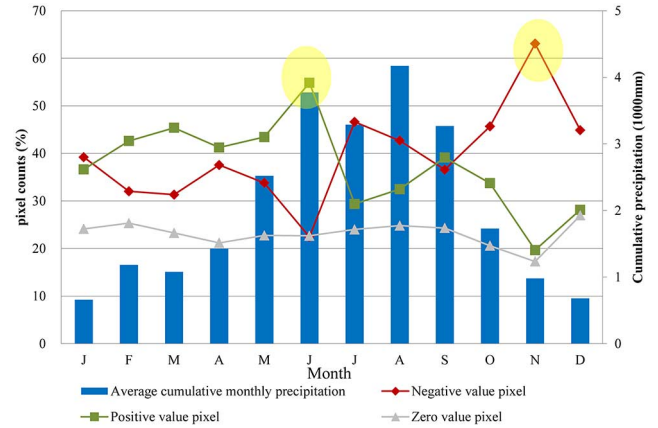


Fig. 8. Monthly relative persistence directional metric  $R$  for Taiwan with relevant 1982–2012 averaged cumulative precipitation.

In addition, a wide range of established trend estimation methods involves regression and breakpoints analysis such as Annual Aggregated Time Series (AAT), Season-Trend Model (STM), Mean Annual Cycle (MAC), and Singular Spectrum Analysis (SSA). Forkel *et al.* [122] argued that interannual variability would influence the accuracy of NDVI trend change detection. Subsequently, such trend estimation methods need to be improved against interannual variability to more accurately quantify the changing trends in ecosystem productivity. Nevertheless, according to the detailed theoretical developing process in [120],  $R$  mainly focuses on detecting the directional change of NDVI time series without involving any estimation methods like regression analysis or breakpoints analysis. Therefore,  $R$  is not constrained by statistical assumptions such as the independence of observations that make  $R$  different from regression and breakpoints analysis.

Generally, positive scores seem to dominate the entire island from January to June, the first half of the year, while negative scores dominate from July to December, the second half of the year. Other than this general pattern, however, monthly spatial variations, such as June and November, stand out as the distinct positive and negative patterns of NDVI (Fig. 7). In June, 55% of pixels return positive  $R$  scores, indicating an increasing pattern of NDVI, whereas 63% of pixels yield negative  $R$  scores in November, representing a decreasing pattern of NDVI (Fig. 8).

Figs. 8 and 9 show monthly variations results of  $R$ . For Taiwan, an average of 23% of pixels show zero scores, whereas 40% of pixels return positive scores and 37% of pixels return negative scores. As stated above, the first half of the year is dominated by an increasing trend of NDVI, whereas a decreasing trend takes over in the second half of the year (Fig. 8). The northern counties [Fig. 9(a)] largely return positive scores, especially in June, when 72% of pixels show positive scores, whereas late summer (July and August) and winter (November to January) return more negative scores. Central counties [Fig. 9(b)] exhibit more pronounced negative scores during the winter months (November–January) and late summer (July–September). Similar negative patterns in the winter months can also be seen in the southern and eastern counties [Fig. 9(c) and (d)], particularly for the eastern

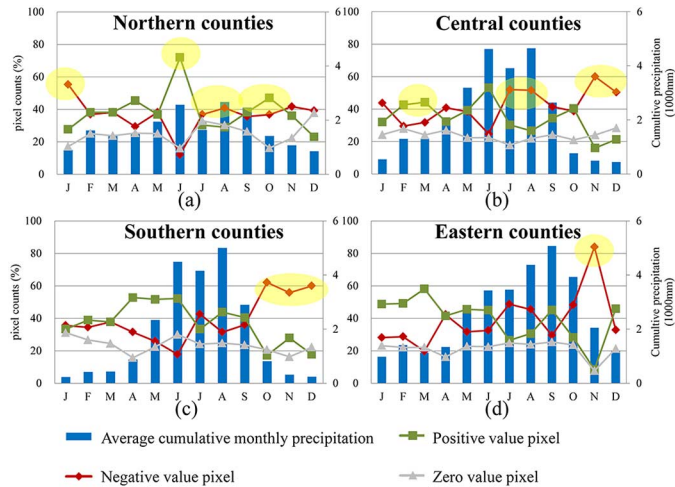


Fig. 9. Monthly pixel percentage of relative directional persistence metric  $R$  with averaged cumulative precipitation. (a) Northern counties. (b) Central counties. (c) Southern counties. (d) Eastern counties. Positive value pixels are shown in green, negative value pixels are shown in red, and zero value pixels are shown in gray.

counties [Fig. 9(d)], where more than 80% of pixels return negative scores in November. Table I and Fig. 10 summarize the seasonal results of  $R$ . Increasing pattern dominate the spring months (March–May) throughout Taiwan [Fig. 10(a)]. From June to August (summer time), the northern and southern counties exhibit an increasing pattern while the central and eastern counties show a decreasing pattern [Fig. 10(b)]. Other than the northern counties, Taiwan illustrates a prevalent decreasing pattern from September to November [Fig. 10(c)]. During the winter months (December–February), with the exception of the eastern counties, the entire island displays a decreasing pattern [Fig. 10(d)].

Among the 20% of pixels with zero score and 80% of pixels with a nonzero score, the percentage of negative scores is particularly high in the southern (51%) and eastern counties (54%). Additionally, Fig. 11 summarizes the results by region and reflects the major disturbance events in Fig. 3. Further regional variation of monthly  $R$  can be found in Figs. 12–16.

Table II lists the critical values of  $R$ . In this study, 31 years of observation yield 30 transitions; thus, a significance level can be chosen to highlight pixels that experienced unusual changes. A detailed description of the process in establishing the relevant statistical theory can be found in [120]. The circles in Fig. 7 identify pixels returning statistically significant scores ( $p = 0.05$ ). Overall, the significantly negative pixels outnumbered positive ones. June is the month with the highest number of significantly positive pixels, and March comes in the second place. The largest amount of significantly negative pixels appears in November, with July coming in second. From a spatial perspective, significantly positive pixels appear in the central and southern counties during the early months and reach their peak in March in the central counties. In June, significantly positive pixels move to the northern counties and become less present for the remainder of the year. Significantly negative pixels concentrate in the northern counties in January and move to the central and southern counties subsequently. Especially in

TABLE I  
 SEASONAL RELATIVE PERSISTENCE DIRECTIONAL METRIC  $R$

County	Month	Negative score pixel %	Positive score pixel %	Zero score pixel %
Northern counties	DJF	44	30	27
	MAM	35	40	25
	JJA	30	44	26
	SON	38	40	22
Central counties	DJF	41	32	27
	MAM	37	39	24
	JJA	43	37	21
	SON	47	30	23
Southern counties	DJF	43	30	27
	MAM	32	47	21
	JJA	30	43	26
	SON	51	29	20
Eastern counties	DJF	30	48	22
	MAM	31	48	20
	JJA	42	34	24
	SON	54	27	19
Taiwan	DJF	39	36	25
	MAM	34	43	22
	JJA	37	39	24
	SON	48	31	21

July, the central counties were dominated by significantly negative pixels and an overwhelmingly negative pattern was evident in the central and eastern counties in November.

D. Pearson’s Product Moment Coefficient

Fig. 17 presents Pearson’s product correlation coefficients between NDVI and four climate variables, including sunshine duration, temperature, precipitation, and cloud amount at a monthly scale suggested by many scholars [63], [71], [123]–[124]. The results show a general positive correlation between NDVI and sunshine duration and temperature, and a general negative correlation between NDVI and precipitation and cloud amount.

An overall positive correlation is observed between sunshine duration and NDVI, which indicates that long sunshine hours benefit the growth of vegetation and yields high NDVI. Statistically, sunshine duration is strongly positively correlated with NDVI in August ( $r = 0.59, p < 0.001$ ), and the remaining months of April, July, September, and October also display a significant positive correlation ( $r > 0.40, p < 0.05$ ). For temperature, a moderate to high significant positive correlation was found during March and August in Taiwan ( $r = 0.47$  and  $0.37$ , respectively,  $p < 0.05$ ). A nonsignificant positive correlation was obtained for other months, and only September and October exhibited a weak negative relationship between temperature and NDVI.

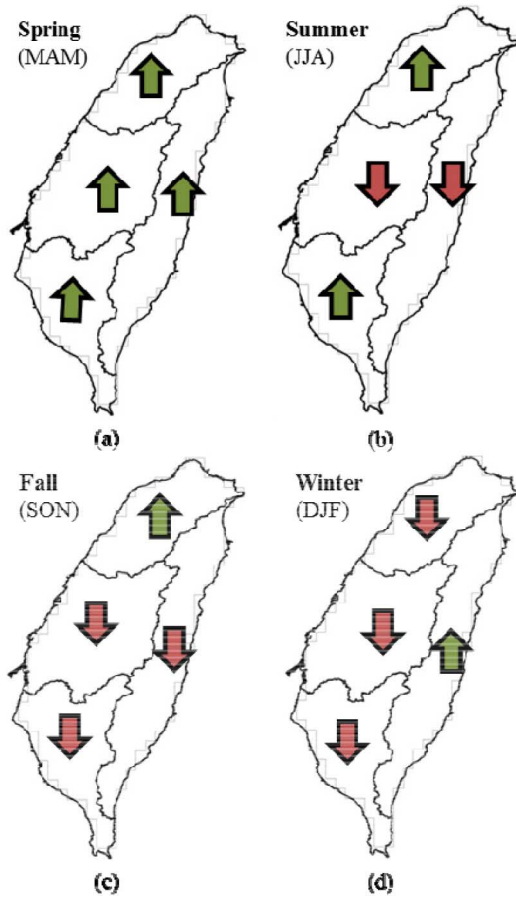


Fig. 10. Seasonal relative persistence directional metric  $R$ . Green (red) arrow represents more positive (negative) score pixels within the particular season and area.

The most surprising result is the general negative relationship between precipitation and NDVI. A strong negative correlation was found between precipitation and NDVI in May ( $r = -0.59, p < 0.001$ ), February, and August ( $r < -0.40, p < 0.05$ ). With the exception of September and December, which show an insignificant positive correlation, all months reveal a negative correlation. Cloud amount shows a consistent negative correlation with NDVI. The negative correlation is particularly strong and statistically significant ( $r < -0.57, p < 0.001$ ) in June and August. April, July, September, and October display weak to moderate negative correlations (but not statistically significant) whereas other months reveal significant negative correlation coefficients ranging from  $-0.35$  to  $-0.55$  ( $p < 0.05$ ).

#### IV. DISCUSSION

##### A. Interannual Variations in NDVI and Climate Variables

A slight increasing NDVI tendency over the study period (1982–2012) can be attributed to the overall forest protection policy in Taiwan. In 1976, the principles for the management of national forest in Taiwan have shifted from timber production to forest protection under the consideration of conservation, sustained yield, and public welfare. By 1990, 99% of the timber supply in Taiwan was imported [125]. Nowadays, the amount of

	North	Central	South	East	TWN
1983	Green	Green	Green	Red	Green
1984	Red	Red	Red	Red	Red
1985	Green	Green	Green	Green	Green
1986	Green	Red	Red	Green	Green
1987	Red	Green	Green	Green	Red
1988	Red	Green	Green	Red	Red
1989	Green	Green	Red	Green	Green
1990	Red	Red	Red	Red	Red
1991	Green	Green	Red	Red	Green
1992	Red	Red	Red	Red	Red
1993	Red	Green	Red	Red	Red
1994	Red	Red	Red	Red	Red
1995	Green	Green	Green	Green	Green
1996	Red	Red	Red	Red	Red
1997	Green	Green	Green	Green	Green
1998	Red	Green	Green	Green	Red
1999	Red	Red	Red	Red	Red
2000	Red	Red	Green	Red	Red
2001	Green	Green	Green	Green	Green
2002	Gray	Red	Red	Green	Red
2003	Red	Red	Red	Red	Red
2004	Green	Green	Green	Green	Green
2005	Red	Green	Green	Red	Red
2006	Green	Green	Green	Green	Green
2007	Green	Green	Red	Green	Green
2008	Green	Green	Green	Green	Green
2009	Green	Green	Green	Green	Green
2010	Red	Green	Red	Red	Red
2011	Green	Red	Green	Red	Red
2012	Red	Red	Green	Red	Red

Fig. 11. Summary of the relative persistence directional metric  $R$ . Green (red) indicates the prevalence of positive (negative) pixels, while gray represents a balance between positive and negative pixels.

logging and forest clearing activities in Taiwan were regulated by law and restricted to certain forest plantation area.

Along with the slightly increasing NDVI over the study period, several fluctuations exist in the timeline [Fig. 3(a)] and several low NDVIs are probably associated with natural disturbances that occurred in Taiwan. For instance, the lowest NDVI recorded in 1984 may link to the flood that occurred in the Mei-Yu season (June) caused by frontal system-related convective activity. This event dropped a maximum of 400 mm of rain within 6 h on northern Taiwan and resulted in serious property and agricultural losses. Additionally, Taiwan is affected by an average of four tropical cyclones per year [126] and many major typhoons have struck Taiwan with devastating damage. These typhoons' impacts were revealed by a decreased NDVI value for the concurrent and even the following years depending on the location-specified vegetation recovery rate [83]. For example, typhoon Herb in July 1996 made landfall as a category

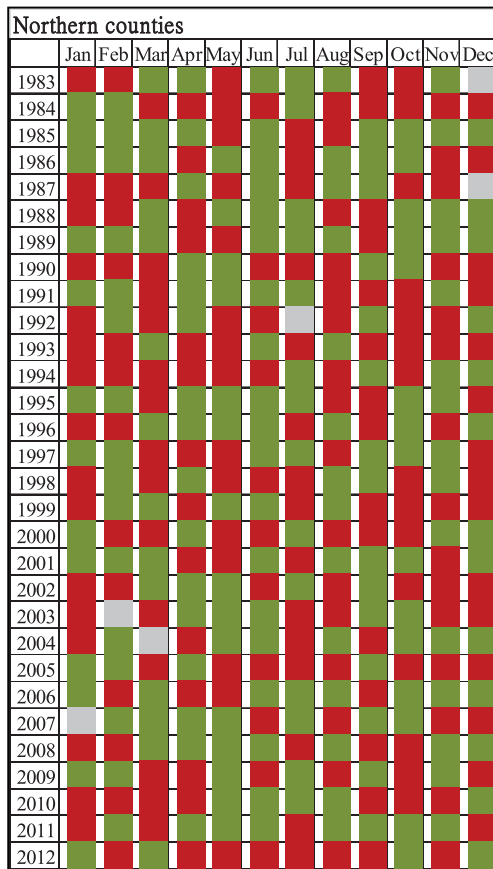


Fig. 12. Monthly relative persistence directional metric *R* by year (the upper bound years are listed) for the northern counties in Taiwan. Green (red) indicates that the positive (negative) value pixels outnumber negative (positive) ones, and gray indicates no differences between the number of positive and negative pixels.

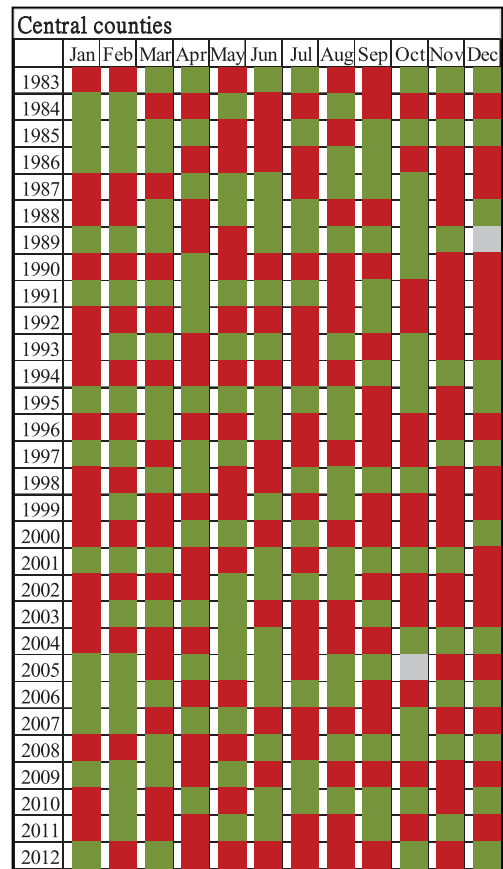


Fig. 13. Monthly relative persistence directional metric *R* by year (the upper bound years are listed) for the central counties in Taiwan. Green (red) indicates that the positive (negative) value pixels outnumber negative (positive) ones, and gray indicates no differences between the number of positive and negative pixels.

3 typhoon, brought almost 2000 mm of rainfall within 48 h, and resulted in 1315 landslides and 20 debris flows [81]. With typhoon Herb, the heaviest damage occurred in central Taiwan [79], and the negative impact can be observed from the decline in the 1996–1997 NDVI values [Fig. 3(a)]. On August 7, 2009, typhoon Morakot struck Taiwan with record-breaking rainfall of over 2800 mm in 100 h, and triggered 22 705 landslides [84], [100]. Over 400 km<sup>2</sup> of land were flooded by the enormous rainfall brought by typhoon Morakot and the effect of rainfall-induced landslides was reflected in the declining NDVI values from 2009 onward. Conversely, 1989 and 1995 reveal relatively high NDVI values without natural disturbances.

Other natural disturbances, such as floods, rainfall-induced landslides, and debris flows, are usually directly influenced by abundant precipitation from tropical cyclones and storms in summer and autumn [127]. Those natural disturbances not only bring severe hazards and threats to human lives and property, but also characterize the structure, function, and dynamics of many tropical and temperate forest ecosystems [79]. As a consequence, the NDVI value can be greatly influenced by natural disturbances.

Moreover, previous studies have shown that rainfall and earthquakes are two main mechanisms that trigger landslides [128]–[130]. In 1999, the Chi-Chi earthquake with a magnitude

of 7.3 on the Richter scale struck Taiwan on September 21. The Chi-Chi earthquake resulted in more than 20 000 sites with a total of 160 km<sup>2</sup> of landslides. The devastating damages to the central Taiwan brought by the Chi-Chi earthquake were possibly associated with the declining NDVI from 1998 to 1999 and even in the following year 2000 [83]. Besides the direct influence from an earthquake, a catastrophic earthquake can intensively disturb ground strata and affect the stability of slopes for a long period [83]. As a consequence, the subsequent rainfall-induced landslides were more likely to increase its density and affected areas [83], [131]. A typical example is the typhoon Toraji in 2001. Typhoon Toraji brought less rainfall than typhoon Herb in 1996, but affected larger area and resulted in the declined NDVI from 2001 onward, because the Chi-Chi earthquake extensively disturbed the surface strata.

Two historically severe droughts were recorded during 1993–1995 and 2002–2004 and were linked closely to precipitation [132]. The prolonged nine-month drought in 1993 was associated with a water shortage caused by the lack of typhoons in the previous year. The drought in 2002–2004 was closely associated with low annual precipitation, 28% less than the long-term average annual precipitation [Fig. 3(b)], and reflected on the low value of NDVI [Fig. 3(a)] [132]. Accompanied with high temperatures, low cloud amount, and long sunshine

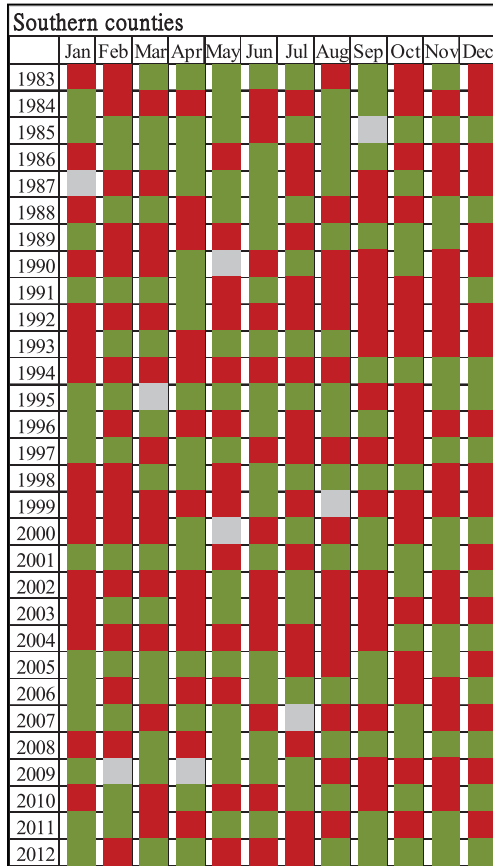


Fig. 14. Monthly relative persistence directional metric  $R$  by year (the upper bound years are listed) for the southern counties in Taiwan. Green (red) indicates that the positive (negative) value pixels outnumber negative (positive) ones, and gray indicates no differences between the number of positive and negative pixels.

duration [Fig. 3(c)–(e)], the years of 2002–2004 were listed as the severest drought years on record in Taiwan in three decades [132].

Furthermore, lower NDVI values found in the early 1980s and 1990s may be connected with the global impact of volcanic eruptions. Volcanic eruptions can enhance the haze effect and lower mean global temperatures by injecting a large amount of suspended ash particles into the upper atmosphere. The large amount of injected suspended ash particles block out solar radiation and result in the reduction of the amount of sunlight reaching the Earth's surface, thus decreasing temperatures globally [133], [134]. The cooling effect from the reduction of sunlight may influence vegetation growth, which may negatively impact NDVI for several years [135]–[137]. In this study, the cooling effect of the 1982 El Chichon eruption and 1991 Mount Pinatubo eruption can be seen in 1982–1984 and 1992–1994 from the lower NDVI value, lower temperature, lower sunshine duration, and higher cloud amount [136], [138] [Fig. 3(b)–(e)].

High precipitation records found in the years 1990, 1998, and 2005 [Fig. 3(b)] were coincident with the findings from [139]. Decreasing trends in sunshine duration in major urban centers were found in [140] from 1898 to 1999; they argued that the trends are most likely caused by an increase in

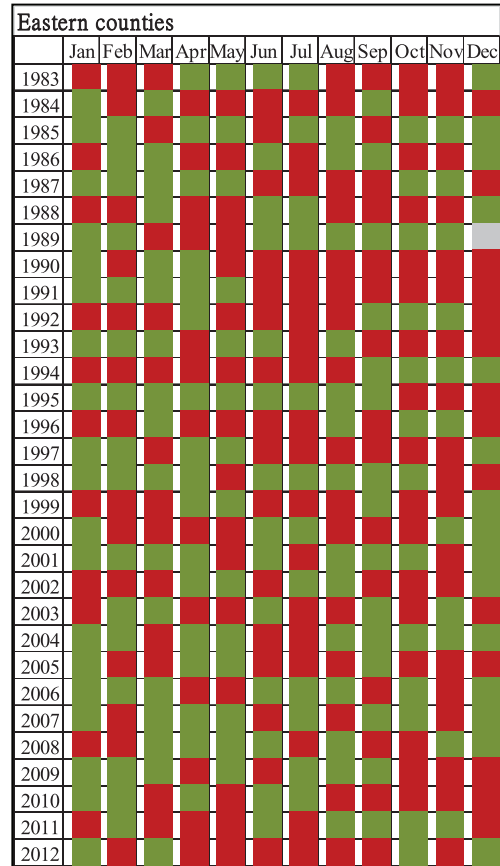


Fig. 15. Monthly relative persistence directional metric  $R$  by year (the upper bound years are listed) for the eastern counties in Taiwan. Green (red) indicates that the positive (negative) value pixels outnumber negative (positive) ones, and gray indicates no differences between the number of positive and negative pixels.

regional clouds and/or cloud albedo as a result of increased anthropogenic aerosols. However, a declining trend of cloud amount [Fig. 3(d)] and a slightly increasing trend of sunshine duration [Fig. 3(e)] are found in this research. The discrepancy between this study and [140] may result from the different temporal data coverage and this study may reflect a fluctuation or a changing point in the long-term pattern found in [140].

Based on the Intergovernmental Panel on Climate Change (IPCC) reports [141], [142], other than the medium confidence (50%) in a warming trend in daily temperature extremes in much of Asia, it is likely (66%–90%) that the frequency of heavy precipitation, namely, the proportion of total rainfall from heavy rainfalls associated with tropical cyclones, will increase in the 21st century over many areas of the globe. According to [143], the annual average temperature of Taiwan has increased approximately 1.4 °C from 1911 to 2009, and the rate of increase is two times faster than global average for the last three decades (1980–2009). Although no significant trend is observed in annual precipitation, an island-wide decrease in precipitation days has been detected on the order of –6 days/decade since the 1980s [143]. Additionally, reference [144] found an upward trend in heavy precipitation (> 10 mm/h) from 1961 to 2005 in Taiwan, while reference [145] suggested that the upward trend is likely associated with

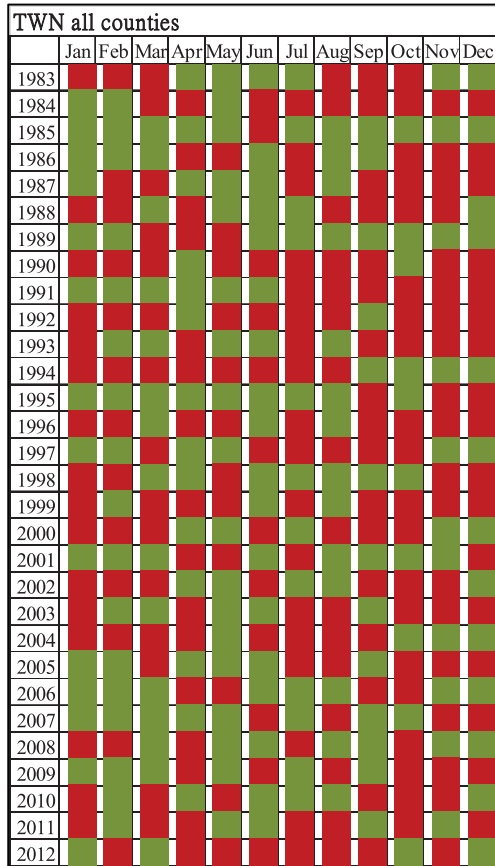


Fig. 16. Relative directional metric  $R$  for Taiwan by year (the upper bound years are listed). Green (red) color represents outnumbered positive (negative) pixels.

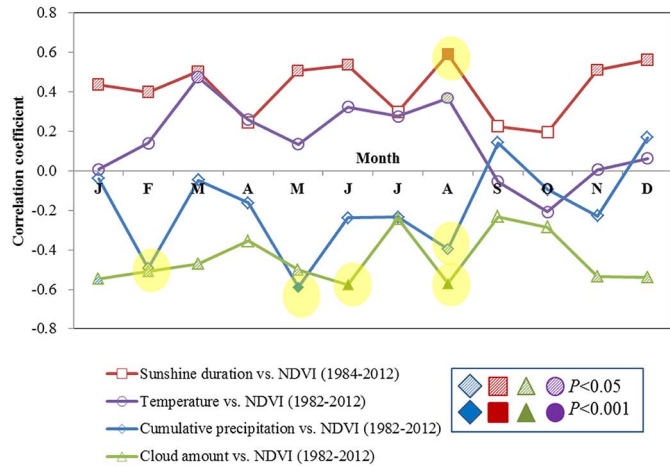


Fig. 17. Pearson product moment correlation coefficients for NDVI with climate variables.

climate change. Moreover, the seasonal typhoon counts in the vicinity of Taiwan have been increasing abruptly since 2000 [146], and the precipitation intensity induced by both typhoons and monsoon systems has increased over the last 60 years [147], [148]; these mechanisms collectively contribute to the upward trend in precipitation intensity. Climate extremes, such as heat waves, extreme precipitation, drought, the intensity of tropical cyclones, and rising sea levels have been observed

TABLE II  
CRITICAL SCORES OF THE RELATIVE DIRECTIONAL PERSISTENCE METRIC  $R$

Significance Level					
	0.005	0.010	0.025	0.050	0.100
score	10	10	8	8	6

The number of observed transitions  $n = 30$  is equal to the total record length of 31 years (1982–2012) minus 1.

worldwide due to their devastating consequences on society and economy [148]. Given the rising temperature, increasing number of typhoons, and intensified typhoon-induced precipitation, Taiwan is facing growing challenges of the influences from global climate change and climate extremes on agriculture, conservation, water resources, socioeconomic activity, and food security.

B. Mean-Variance Analysis

The slightly increasing NDVI mean value from the 1980s to the 2000s found here agrees with the results of [23] and [149]. Additionally, the highest variance values appearing during the 1990s may imply a higher degree of natural fluctuation in the landscape. Based on more than 100 years of annual cumulative precipitation data (1911–2009) and the base line year’s average precipitation (1980–1999), reference [132] noted that the fluctuation (above and below average) occurred three times in the last 50 years (1960–2009); however, the fluctuation became more frequent after the late 1980s, occurring three times within 15 years (1985–2000). After 2000, the average precipitation is observed with less frequent fluctuations. Due to the close relationship between precipitation and NDVI [1], [23], [55], [75], it is reasonable to infer that the fluctuation of the annual cumulative precipitation has the potential to influence the NDVI variance values observed in Taiwan. In the context of global climate change, precipitation patterns are expected to be more variable. Thus, the associated vegetation dynamics and ecosystems functions would pose serious challenges, such as agricultural and conservational management, for policy makers and stakeholders in Taiwan.

C. Relative Directional Persistence Metric

A possible interpretation of the increasing pattern of NDVI for the first half of the year may lie in the increasing observed precipitation [96], [150], and the decreasing pattern of NDVI may be associated with typhoon-related disturbances such as abundant rainfall, landslides, and debris flows during the typhoon season (July–September). Although further investigation is needed, the decreasing pattern during the winter months and the distinct declining pattern in November may be related to large-scale atmospheric circulations such as the ENSO or the Pacific decadal oscillation (PDO) [77], [151], [152].

In Fig. 11, the negative impact from the Mei-Yu induced flood (June) was associated with the low NDVI value in 1984 and results in the outnumbered negative pixels. In addition,

typhoon-related disturbances such as rainfall-induced landslides and debris flows are speculated to influence the NDVI value negatively. Evidence can be seen in the year and even the following year of major typhoon event such as in 1996 (typhoon Herb) and in 2009 (typhoon Morakot). Moreover, the Chi-Chi earthquake with subsequent landslides intensively disturbed the landscape results in the low NDVI value in 1999–2000. Furthermore, the adverse effects of drought (1992–1994 and 2002–2004) and volcanic eruptions (1982–1984 and 1992–1994) to NDVI contribute to unfavorable conditions for vegetation growth. Overall, for the entire island throughout the 31-year study period (1982–2012), 18 years return more negative scores indicating a prevalent decreasing NDVI pattern over these three decades. The northern counties show an approximately balanced situation (14 negative years with 15 positive years and one zero year), and negative patterns are prevalent among other regions.

Although the total number of significant pixels (negative and positive) account for a small proportion (1%–2%) of the whole, it is noteworthy that the number of positive pixels exceeds that of the negative pixels from January to June, whereas the situation is reversed from July to December. Indeed, these results declare that Taiwan has two distinct patterns of NDVI: 1) an increasing pattern in the first half of the year and 2) a decreasing pattern in the second half of the year, suggesting a more enhanced seasonal variation. This enhanced seasonal variation also corresponds to the original  $R$  results (Figs. 7 and 8) and the observational evidence [132], [153].

Nevertheless, these significant pixels are not showing clear groupings (except November), which suggest that localized phenomena may play an important role on these unexpected changes. This situation also reflects the terrain characteristics of Taiwan, resulting in a high level of local vegetation variations. Thus, more local or downscaled remote sensing information are needed to further investigate the underlying phenomena.

Many studies focusing on precipitation patterns support the regional results of  $R$ . The increasing NDVI pattern discovered in the northern counties coincides with the findings of [132] as an observed statistically significant increase in precipitation in the Taipei weather station, located in the northern part of Taiwan (25°2' 23'N, 121°30' 24'E), from 1911 to 2009. In addition, reference [96] also discerned an increasing precipitation trend of 3–4 mm/year in northeastern Taiwan from 1897 to 1999 and this upward pattern was confirmed again in [102] and [154]. Furthermore, due to the positive correlation between the PDO and spring rainfall in northern Taiwan, the positive PDO signal from 1977 through the mid-1990s resulted in more spring rain in northern Taiwan, which is reflected in the increasing pattern of NDVI [151].

The decreasing NDVI pattern exhibited in the central and southern counties seems to be at odds with previous research results [96], [102], which show a declining precipitation tendency in central and southern Taiwan. Additionally, a rational explanation for the observed decreasing NDVI pattern may link closely to the observed declining annual number of precipitation days [96], [132], [154]. Reference [132] found a general declining trend in precipitation days from 1911 to 2009, where the trend was statistically significant in the southern and eastern

stations for the last 30 years. Moreover, because no sufficient statistical evidence discerns a long-term annual precipitation trend [132], the general decreasing trend in precipitation days implies that the precipitation intensity may have increased in compensation for the decreased rainy days [96], [132], [144]. As such, the impact of intensified precipitation may be associated with the decreasing NDVI pattern. According to the limited space and the scope of this study, the impacts of intensified precipitation will not be discussed.

Given that the water supply is critical for plant growth, precipitation usually shows a considerable positive correlation with NDVI values [6], [10], [16], [19], [51], [61], [73], [155]. Other than the natural disturbances resulting in negatively impact on NDVI values, such as floods, landslides, or debris flows triggered by excessive precipitation, some scholars argued that there is a location-dependent negative correlation between NDVI and precipitation. Reference [60] reported a negative correlation of NDVI and precipitation in northeast China based on the hypothesis that precipitation causes more clouds to appear and then reduces the incident radiation, thus hindering photosynthesis. In addition, reference [149] reported that increasing rainfall could also shorten the growing season and reduce the incoming solar radiation, thus decreasing NDVI in rainy regions. Moreover, heavy rainfall accompanied by a surplus of surface runoff could carry the seeds of former early summer species away or induce them to root or even germinate prematurely [156]. This could result in seed loss or poor/late filling of seeds, thus indirectly affecting the seed bank and eventually influencing the NDVI value [157]. However, the correlation may be location dependent [158]; thus, in order to investigate the correlation between NDVI, precipitation, and other climate variables, including temperature, cloud amount, and sunshine duration, Pearson's product correlation coefficient analysis is carried out.

#### D. Pearson's Product Moment Coefficient

An overall positive correlation has been observed between NDVI and sunshine duration and temperature, whereas precipitation and cloud amount are negatively correlated with NDVI. Given the observed increasing (decreasing) precipitation pattern for the northern (southern and eastern) counties [96], [102], [132], these correlation results are especially important because they provide an opportunity to infer their relationship and thereby forecast their occurrence and impacts under changing climate conditions [159]. According to the recently released IPCC AR5 downscaled model projections [132], approximately half of the models predict decreasing winter precipitation (–3% to –22%) in Taiwan. Additionally, more than 75% of the models predict increasing summer precipitation (+2% to +26%) in Taiwan. These model projections indicate an increasing range between wet and dry season precipitations, which is also supported by a global scaled research conducted in [160]. Moreover, the increased range between wet and dry season precipitations is evident in the increasing occurrences of extreme dry spells during the winter months [161] and extreme heavy precipitation during the summer months in Taiwan [153]. Together with the results from the relative

directional persistence metric  $R$ , this enhanced seasonal variation is confirmed again. Hence, the enhanced seasonal variation is especially vital for Taiwan as it may intensify the positive and negative NDVI patterns and pose extra pressure in various aspects, such as rain-fed agricultural practices, conservation practices, water resource management, socioeconomic activities, and food security in Taiwan.

## V. CONCLUSION

This study demonstrates a novel approach that combines temporal and spatial analysis employing a remotely sensed VI time series. Specifically, MVA and relative directional persistence analysis are applied to 31 years (1982–2012) of monthly AVHRR-derived NDVI in Taiwan. The statistical test along with the relative directional persistence metric permits the identification of changes that are different from what might be expected at random. Moreover, a set of climate variables, namely, precipitation, temperature, sunshine duration, and cloud amount, are analyzed using Pearson’s product moment correlation analysis to assess the relationship between NDVI and climate variables. Three research questions and their corresponding findings are described in the following.

*What is the overall long-term NDVI pattern in Taiwan between 1982 and 2012?* The results from MVA provide insight into the long-term NDVI pattern by analyzing the temporal changes from the value of mean and variance. The mean value of NDVI increases slightly from the 1980s to the 2000s, and the variance values are relatively higher during the 1990s and lower during the 2000s. Similar patterns are found in the annual, spring/summer (March–August), and fall/winter (September–February) data, indicating common NDVI dynamics. The increasing mean and fluctuating variance may be associated with the observed precipitation variation and natural disturbances [78], [81], [83], [100], [126], [127], [131]–[133], [136], [138], [162]–[164].

*How is the spatial pattern of monthly NDVI varied in Taiwan?* The relative directional persistence metric  $R$  provides a new perspective by allowing comparisons to observations from the preceding year in order to capture the directional increase or decrease in NDVI. From the monthly results of  $R$ , it is clear that there are two distinct NDVI patterns: 1) an increasing pattern for the first half of the year and 2) a decreasing NDVI pattern for the second half of the year. Additionally, June and November stand out as their distinct positive and negative patterns may correspond to the observed enhanced seasonal variation [132], [153]. Moreover, decreasing patterns of NDVI with regional variations have been discerned in 18 of the 31 study years. The northern counties exhibit an increasing NDVI pattern, whereas the central and southern counties experience a decreasing trend. The two distinct patterns of NDVI are emphasized again by the statistically significant test as positive statistically significant pixels outnumbered negative ones from January to June, with the situation being reversed from July to December.

*What is the relationship between NDVI and climate variables, such as precipitation and temperature?* Pearson’s

product moment coefficient analysis was carried out to assess the relationship between NDVI and a set of climate variables, namely, precipitation, temperature, sunshine duration, and cloud amount. The overall results show that sunshine duration and temperature are positively correlated with NDVI, whereas precipitation and cloud amount are negatively correlated with NDVI. Monthly variations can be seen from their statistical significance levels. Almost all months show a statistically significant positive correlation between NDVI and sunshine duration, whereas temperature displays a significant positive correlation in March and August. Statistically significant negative correlations are found between precipitation and NDVI in February, May, and August, whereas cloud amount expresses a significant negative relationship with NDVI in almost all months. In the context of global environmental change, this correlation analysis highlights the importance of each climate variable’s contribution to NDVI and indicates an accurate direction for future climate predictions.

The regional variation of the NDVI pattern derived from the relative directional persistence metric  $R$  corresponds well with the observed precipitation pattern, indicating a close relationship between NDVI and precipitation. Precipitation variability alone, however, does not provide a complete picture of NDVI drivers in Taiwan. Other factors, such as the ratio of vegetation productivity to annual precipitation [rain use efficiency (RUE)], soil type, soil moisture, and rainfall-induced natural disasters including landslides, debris flow, and floods, all play important roles in NDVI. Additionally, the societal demands of an increasing population and the associated economic development may lead to various LULCC through urbanization, agriculture, and industrial activity at different spatial and temporal scales. Thus, the identified significant pixels from the relative directional persistence metric  $R$  may convey important messages concerning localized LULCC or reflect the influence from large-scale atmospheric phenomena such as ENSO and PDO [75].

This study illuminates the long-term spatial and temporal NDVI patterns from 1982 to 2012 for Taiwan. The observed marked regional variations indicate that Taiwan’s diverse ecosystem may correspond to abiotic–biotic factors at different temporal and spatial scales. A better understanding of Taiwan’s long-term vegetation dynamics may have very important implications in various aspects such as agricultural practices, conservation practices, water resource management, socioeconomic activities, and food security. In addition to considering future climate variability and possible climate change directions, this study not only sheds light on the long-term patterns of Taiwan’s vegetation dynamics, but also provides valuable information that would benefit the establishment of proper mitigation guides and adaptation strategies for Taiwan.

## REFERENCES

- [1] G. Bao, Z. Qin, Y. Bao, Y. Zhou, W. Li, and A. Sanjjav, “NDVI-Based long-term vegetation dynamics and its response to climatic change in the mongolian plateau,” *Remote Sens.*, vol. 6, pp. 8337–8358, 2014.
- [2] P. S. Beck, C. Atzberger, K. A. Høgda, B. Johansen, and A. K. Skidmore, “Improved monitoring of vegetation dynamics at very high latitudes: A new method using MODIS NDVI,” *Remote Sens. Environ.*, vol. 100, pp. 321–334, 2006.

- [3] A. Begue, E. Vintrou, D. Ruelland, M. Claden, and N. Dessay, "Can a 25-year trend in Soudano-Sahelian vegetation dynamics be interpreted in terms of land use change? A remote sensing approach," *Global Environ. Change*, vol. 21, pp. 413–420, 2011.
- [4] C. Gouveia, R. M. Trigo, C. C. DaCamara, R. Libonati, and J. Pereira, "The north atlantic oscillation and european vegetation dynamics," *Int. J. Climatol.*, vol. 28, pp. 1835–1847, 2008.
- [5] J. Wang, J. Meng, and Y. Cai, "Assessing vegetation dynamics impacted by climate change in the southwestern karst region of China with AVHRR NDVI and AVHRR NPP time series," *Environ. Geol.*, vol. 54, pp. 1185–1195, 2008.
- [6] J. Fang, S. Piao, Z. Tang, C. Peng, and W. Ji, "Interannual variability in net primary production and precipitation," *Science*, vol. 293, p. 1723, Sep. 7, 2001.
- [7] A. Hoscoilo *et al.*, "A conceptual model for assessing rainfall and vegetation trends in sub-Saharan Africa from satellite data," *Int. J. Climatol.*, vol. 35, pp. 3582–3592, 2014.
- [8] A. Karnieli *et al.*, "Use of NDVI and land surface temperature for drought assessment: merits and limitations," *J. Clim.*, vol. 23, pp. 618–633, 2010.
- [9] M. Yang and R. Sykes, "Trophic-dynamic modeling in a shallow eutrophic river ecosystem," *Ecol. Modell.*, vol. 105, pp. 129–139, 1998.
- [10] X. Zhao, K. Tan, S. Zhao, and J. Fang, "Changing climate affects vegetation growth in the arid region of the northwestern China," *J. Arid Environ.*, vol. 75, pp. 946–952, 2011.
- [11] M. A. Campo-Bescós, R. Muñoz-Carpena, J. Southworth, L. Zhu, P. R. Waylen, and E. Bunting, "Combined spatial and temporal effects of environmental controls on long-term monthly NDVI in the southern Africa Savanna," *Remote Sens.*, vol. 5, pp. 6513–6538, 2013.
- [12] K. Jia *et al.*, "Fractional forest cover changes in northeast China from 1982 to 2011 and its relationship with climatic variations," *IEEE J. Sel. Topics Appl. Earth Observ. Remote Sens.*, vol. 8, pp. 775–783, 2015.
- [13] J. Bai, L. Di, and J. Bai, "NDVI and regional climate variation since the implementation of revegetation program in northern Shaanxi Province, China," *IEEE J. Sel. Topics Appl. Earth Observ. Remote Sens.*, vol. 7, pp. 4581–4588, 2014.
- [14] C. Chang, T. Lin, S. Wang, and M. A. Vadeboncoeur, "Assessing growing season beginning and end dates and their relation to climate in Taiwan using satellite data," *Int. J. Remote Sens.*, vol. 32, pp. 5035–5058, 2011.
- [15] Q. Ge, X. Zhang, and J. Zheng, "Simulated effects of vegetation increase/decrease on temperature changes from 1982 to 2000 across the Eastern China," *Int. J. Climatol.*, vol. 34, pp. 187–196, 2014.
- [16] K. Ichii, A. Kawabata, and Y. Yamaguchi, "Global correlation analysis for NDVI and climatic variables and NDVI trends: 1982–1990," *Int. J. Remote Sens.*, vol. 23, pp. 3873–3878, 2002.
- [17] L. Jarlan *et al.*, "Spatio-temporal variability of vegetation cover over Morocco (1982–2008): Linkages with large scale climate and predictability," *Int. J. Climatol.*, vol. 34, pp. 1245–1261, 2014.
- [18] Y. H. Kerr, J. Imbernon, G. Dedieu, O. Hautecoeur, J. Lagouarde, and B. Seguin, "NOAA AVHRR and its uses for rainfall and evapotranspiration monitoring," *Int. J. Remote Sens.*, vol. 10, pp. 847–854, 1989.
- [19] S. Piao, A. Mohammat, J. Fang, Q. Cai, and J. Feng, "NDVI-based increase in growth of temperate grasslands and its responses to climate changes in China," *Global Environ. Change*, vol. 16, pp. 340–348, 2006.
- [20] J. A. Sobrino and Y. Julien, "Trend analysis of global MODIS-Terra vegetation indices and land surface temperature between 2000 and 2011," *IEEE J. Sel. Topics Appl. Earth Observ. Remote Sens.*, vol. 6, pp. 2139–2145, 2013.
- [21] J. Wang, K. Price, and P. Rich, "Spatial patterns of NDVI in response to precipitation and temperature in the central Great Plains," *Int. J. Remote Sens.*, vol. 22, pp. 3827–3844, 2001.
- [22] L. Yang, B. K. Wylie, L. L. Tieszen, and B. C. Reed, "An analysis of relationships among climate forcing and time-integrated NDVI of grasslands over the US northern and central Great Plains," *Remote Sens. Environ.*, vol. 65, pp. 25–37, 1998.
- [23] B. Chen *et al.*, "Changes in vegetation photosynthetic activity trends across the Asia-Pacific region over the last three decades," *Remote Sens. Environ.*, vol. 144, pp. 28–41, 2014.
- [24] R. Nayak, N. Patel, and V. Dadhwal, "Inter-annual variability and climate control of terrestrial net primary productivity over India," *Int. J. Climatol.*, vol. 33, pp. 132–142, 2013.
- [25] N. Son, C. Chen, C. Chen, V. Minh, and N. Trung, "A comparative analysis of multitemporal MODIS EVI and NDVI data for large-scale rice yield estimation," *Agric. For. Meteorol.*, vol. 197, pp. 52–64, 2014.
- [26] J. Wang, P. Rich, and K. Price, "Temporal responses of NDVI to precipitation and temperature in the central Great Plains, USA," *Int. J. Remote Sens.*, vol. 24, pp. 2345–2364, 2003.
- [27] Q. Zhang *et al.*, "Estimation of crop gross primary production (GPP): II. Do scaled MODIS vegetation indices improve performance?," *Agric. For. Meteorol.*, vol. 200, pp. 1–8, 2015.
- [28] L. Zhu and J. Southworth, "Disentangling the relationships between net primary production and precipitation in southern Africa savannas using satellite observations from 1982 to 2010," *Remote Sens.*, vol. 5, pp. 3803–3825, 2013.
- [29] R. DeFries and J. Townshend, "NDVI-derived land cover classifications at a global scale," *Int. J. Remote Sens.*, vol. 15, pp. 3567–3586, 1994.
- [30] R. S. Lunetta, J. F. Knight, J. Ediriwickrema, J. G. Lyon, and L. D. Worthy, "Land-cover change detection using multi-temporal MODIS NDVI data," *Remote Sens. Environ.*, vol. 105, pp. 142–154, 2006.
- [31] Z. Xue, P. Du, and L. Feng, "Phenology-driven land cover classification and trend analysis Based on long-term remote sensing image series," *IEEE J. Sel. Topics Appl. Earth Observ. Remote Sens.*, vol. 7, pp. 1142–1156, 2014.
- [32] M. Yang, C. J. Merry, and R. M. Sykes, "Integration of water quality modeling, remote sensing, and GIS," *J. Amer. Water Resour. Assoc.*, vol. 35, pp. 253–263, 1999.
- [33] X. Zhu, W. Zhu, J. Zhang, and Y. Pan, "Mapping irrigated areas in China from remote sensing and statistical data," *IEEE J. Sel. Topics Appl. Earth Observ. Remote Sens.*, vol. 7, pp. 4490–4504, 2014.
- [34] R. Cao, J. Chen, M. Shen, and Y. Tang, "An improved logistic method for detecting spring vegetation phenology in grasslands from MODIS EVI time-series data," *Agric. For. Meteorol.*, vol. 200, pp. 9–20, 2015.
- [35] N. Cong *et al.*, "Changes in satellite-derived spring vegetation green-up date and its linkage to climate in China from 1982 to 2010: A multimethod analysis," *Global Change Biol.*, vol. 19, pp. 881–891, 2013.
- [36] R. Latifovic and D. Pouliot, "Monitoring cumulative long-term vegetation changes over the Athabasca oil sands region," *IEEE J. Sel. Topics Appl. Earth Observ. Remote Sens.*, vol. 7, pp. 3380–3392, 2014.
- [37] X. Luo, X. Chen, L. Wang, L. Xu, and Y. Tian, "Modeling and predicting spring land surface phenology of the deciduous broadleaf forest in northern China," *Agric. For. Meteorol.*, vol. 198, pp. 33–41, 2014.
- [38] A. D. Richardson, T. F. Keenan, M. Migliavacca, Y. Ryu, O. Sonnentag, and M. Toomey, "Climate change, phenology, and phenological control of vegetation feedbacks to the climate system," *Agric. For. Meteorol.*, vol. 169, pp. 156–173, 2013.
- [39] M. Shen, Y. Tang, J. Chen, X. Zhu, and Y. Zheng, "Influences of temperature and precipitation before the growing season on spring phenology in grasslands of the central and eastern Qinghai-Tibetan Plateau," *Agric. For. Meteorol.*, vol. 151, pp. 1711–1722, 2011.
- [40] R. Suzuki, T. Nomaki, and T. Yasunari, "Spatial distribution and its seasonality of satellite-derived vegetation index (NDVI) and climate in Siberia," *Int. J. Climatol.*, vol. 21, pp. 1321–1335, 2001.
- [41] H. Wang, D. Liu, H. Lin, A. Montenegro, and X. Zhu, "NDVI and vegetation phenology dynamics under the influence of sunshine duration on the Tibetan plateau," *Int. J. Climatol.*, vol. 35, pp. 687–698, 2015.
- [42] X. Zhang *et al.*, "Monitoring vegetation phenology using MODIS," *Remote Sens. Environ.*, vol. 84, pp. 471–475, 2003.
- [43] Y. Gu, J. F. Brown, J. P. Verdin, and B. Wardlow, "A five-year analysis of MODIS NDVI and NDWI for grassland drought assessment over the central Great Plains of the United States," *Geophys. Res. Lett.*, vol. 34, no. 6, pp. 1–6, 2007, article id L06407.
- [44] W. T. Liu, O. Massambani, and C. A. Nobre, "Satellite recorded vegetation response to drought in Brazil," *Int. J. Climatol.*, vol. 14, pp. 343–354, 1994.
- [45] C. Peng, M. Deng, and L. Di, "Relationships between remote-sensing-based agricultural drought indicators and root zone soil moisture: A comparative study of Iowa," *IEEE J. Sel. Topics Appl. Earth Observ. Remote Sens.*, vol. 7, pp. 4572–4580, 2014.
- [46] A. J. Peters, E. A. Walter-Shea, L. Ji, A. Vina, M. Hayes, and M. D. Svoboda, "Drought monitoring with NDVI-based standardized vegetation index," *Photogramm. Eng. Remote Sens.*, vol. 68, pp. 71–75, 2002.
- [47] D. Sun and M. Kafatos, "Note on the NDVI-LST relationship and the use of temperature-related drought indices over North America," *Geophys. Res. Lett.*, vol. 34, pp. 1–4, 2007, article id L24406.
- [48] R. M. Trigo, C. M. Gouveia, and D. Barriopedro, "The intense 2007–2009 drought in the Fertile Crescent: Impacts and associated atmospheric circulation," *Agric. For. Meteorol.*, vol. 150, pp. 1245–1257, 2010.

[49] Z. G. Bai, D. L. Dent, L. Olsson, and M. E. Schaepman, "Proxy global assessment of land degradation," *Soil Use Manage.*, vol. 24, pp. 223–234, 2008.

[50] R. de Jong, S. de Bruin, A. de Wit, M. E. Schaepman, and D. L. Dent, "Analysis of monotonic greening and browning trends from global NDVI time-series," *Remote Sens. Environ.*, vol. 115, pp. 692–702, 2011.

[51] R. Fensholt, K. Rasmussen, P. Kaspersen, S. Huber, S. Horion, and E. Swinnen, "Assessing land degradation/recovery in the African Sahel from long-term earth observation based primary productivity and precipitation relationships," *Remote Sens.*, vol. 5, pp. 664–686, 2013.

[52] D. Helman, I. M. Lensky, A. Mussery, and S. Leu, "Rehabilitating degraded drylands by creating woodland islets: Assessing long-term effects on aboveground productivity and soil fertility," *Agric. For. Meteorol.*, vol. 195, pp. 52–60, 2014.

[53] J. Hill, M. Stellmes, T. Udelhoven, A. Röder, and S. Sommer, "Mediterranean desertification and land degradation: Mapping related land use change syndromes based on satellite observations," *Global Planet. Chang.*, vol. 64, pp. 146–157, 2008.

[54] K. Wessels, F. Van Den Bergh, and R. Scholes, "Limits to detectability of land degradation by trend analysis of vegetation index data," *Remote Sens. Environ.*, vol. 125, pp. 10–22, 2012.

[55] A. Buyantuyev and J. Wu, "Urbanization diversifies land surface phenology in arid environments: interactions among vegetation, climatic variation, and land use pattern in the Phoenix metropolitan region, USA," *Landscape Urban Plann.*, vol. 105, pp. 149–159, 2012.

[56] M. Che *et al.*, "Spatial and temporal variations in the end date of the vegetation growing season throughout the Qinghai–Tibetan Plateau from 1982 to 2011," *Agric. For. Meteorol.*, vol. 189, pp. 81–90, 2014.

[57] B. Chen *et al.*, "The impact of climate change and anthropogenic activities on alpine grassland over the Qinghai–Tibet Plateau," *Agric. For. Meteorol.*, vol. 189, pp. 11–18, 2014.

[58] Z. Li and X. Guo, "Detecting climate effects on vegetation in northern mixed prairie using NOAA AVHRR 1-km time-series NDVI data," *Remote Sens.*, vol. 4, pp. 120–134, 2012.

[59] Y. Liu, X. Wang, M. Guo, H. Tani, N. Matsuoka, and S. Matsumura, "Spatial and temporal relationships among NDVI, climate factors, and land cover changes in Northeast Asia from 1982 to 2009," *GIScience Remote Sens.*, vol. 48, pp. 371–393, 2011.

[60] D. Mao, Z. Wang, L. Luo, and C. Ren, "Integrating AVHRR and MODIS data to monitor NDVI changes and their relationships with climatic parameters in Northeast China," *Int. J. Appl. Earth Observ. Geoinf.*, vol. 18, pp. 528–536, 2012.

[61] N. Nezhlin, A. Kostianoy, and B. Li, "Inter-annual variability and interaction of remote-sensed vegetation index and atmospheric precipitation in the Aral Sea region," *J. Arid Environ.*, vol. 62, pp. 677–700, 2005.

[62] V. K. Prasad, K. Badarinath, and A. Eaturu, "Effects of precipitation, temperature and topographic parameters on evergreen vegetation greenery in the Western Ghats, India," *Int. J. Climatol.*, vol. 28, pp. 1807–1819, 2008.

[63] V. K. Prasad, K. Badarinath, and A. Eaturu, "Spatial patterns of vegetation phenology metrics and related climatic controls of eight contrasting forest types in India analysis from remote sensing datasets," *Theory Appl. Climatol.*, vol. 89, pp. 95–107, 2007.

[64] A. Ramos *et al.*, "Seasonal patterns of Mediterranean evergreen woodlands (Montado) are explained by long-term precipitation," *Agric. For. Meteorol.*, vol. 202, pp. 44–50, 2015.

[65] G. Xu *et al.*, "Changes in vegetation growth dynamics and relations with climate over China's Landmass from 1982 to 2011," *Remote Sens.*, vol. 6, pp. 3263–3283, 2014.

[66] F. Yan, B. Wu, and Y. Wang, "Estimating spatiotemporal patterns of aboveground biomass using Landsat TM and MODIS images in the Mu Us Sandy Land, China," *Agric. For. Meteorol.*, vol. 200, pp. 119–128, 2015.

[67] X. Chen, B. Hu, and R. Yu, "Spatial and temporal variation of phenological growing season and climate change impacts in temperate eastern China," *Global Change Biol.*, vol. 11, pp. 1118–1130, 2005.

[68] C. Gibbes, J. Southworth, P. Waylen, and B. Child, "Climate variability as a dominant driver of post-disturbance savanna dynamics," *Appl. Geogr.*, vol. 53, pp. 389–401, 2014.

[69] N. Martiny, P. Camberlin, Y. Richard, and N. Philippon, "Compared regimes of NDVI and rainfall in semi-arid regions of Africa," *Int. J. Remote Sens.*, vol. 27, pp. 5201–5223, 2006.

[70] M. Rahman, D. Lamb, and J. Stanley, "The impact of solar illumination angle when using active optical sensing of NDVI to infer fAPAR in a pasture canopy," *Agric. For. Meteorol.*, vol. 202, pp. 39–43, 2015.

[71] R. Suzuki, J. Xu, and K. Motoya, "Global analyses of satellite-derived vegetation index related to climatological wetness and warmth," *Int. J. Climatol.*, vol. 26, pp. 425–438, 2006.

[72] A. De Roo, G. Schmuck, V. Perdigao, and J. Thielen, "The influence of historic land use changes and future planned land use scenarios on floods in the Oder catchment," *Phys. Chem. Earth, Parts A/B/C*, vol. 28, pp. 1291–1300, 2003.

[73] A. Kawabata, K. Ichii, and Y. Yamaguchi, "Global monitoring of interannual changes in vegetation activities using NDVI and its relationships to temperature and precipitation," *Int. J. Remote Sens.*, vol. 22, pp. 1377–1382, 2001.

[74] S. Nicholson and T. Farrar, "The influence of soil type on the relationships between NDVI, rainfall, and soil moisture in semi-arid Botswana. I. NDVI response to rainfall," *Remote Sens. Environ.*, vol. 50, pp. 107–120, 1994.

[75] C. Chang, S. Wang, M. A. Vadeboncoeur, and T. Lin, "Relating vegetation dynamics to temperature and precipitation at monthly and annual timescales in Taiwan using MODIS vegetation indices," *Int. J. Remote Sens.*, vol. 35, pp. 598–620, 2014.

[76] T. Lei, S. Wan, and T. Chou, "The comparison of PCA and discrete rough set for feature extraction of remote sensing image classification—A case study on rice classification, Taiwan," *Comput. Geosci.*, vol. 12, pp. 1–14, 2008.

[77] R. Wu, Z. Hu, and B. P. Kirtman, "Evolution of ENSO-related rainfall anomalies in East Asia," *J. Clim.*, vol. 16, pp. 3742–3758, 2003.

[78] Y. Kuo, M. Lee, and M. Lu, "Association of Taiwan's rainfall patterns with large-scale oceanic and atmospheric phenomena," *Adv. Meteorol.*, vol. 2015, 2015.

[79] M. Lee, T. Lin, M. A. Vadeboncoeur, and J. Hwong, "Remote sensing assessment of forest damage in relation to the 1996 strong typhoon Herb at lienhuachi experimental forest, Taiwan," *For. Ecol. Manage.*, vol. 255, pp. 3297–3306, 2008.

[80] M. D. Yang, Y. F. Yang, T. C. Su, and K. S. Huang, "An efficient fitness function in genetic algorithm classifier for Landuse recognition on satellite images," *Sci. World J.*, vol. 2014, pp. 1–12, 2014, article id 264512.

[81] M. Lin and F. Jeng, "Characteristics of hazards induced by extremely heavy rainfall in Central Taiwan—Typhoon Herb," *Eng. Geol.*, vol. 58, pp. 191–207, 2000.

[82] M. Yang, "A genetic algorithm (GA) based automated classifier for remote sensing imagery," *Can. J. Remote Sens.*, vol. 33, pp. 203–213, 2007.

[83] W. Lin, C. Lin, and W. Chou, "Assessment of vegetation recovery and soil erosion at landslides caused by a catastrophic earthquake: A case study in Central Taiwan," *Ecol. Eng.*, vol. 28, pp. 79–89, 2006.

[84] F. Tsai, J. Hwang, L. Chen, and T. Lin, "Post-disaster assessment of landslides in southern Taiwan after 2009 Typhoon Morakot using remote sensing and spatial analysis," *Nat. Hazards Earth Syst. Sci.*, vol. 10, pp. 2179–2190, 2010.

[85] M. Yang, T. Su, C. Hsu, K. Chang, and A. Wu, "Mapping of the 26 December 2004 tsunami disaster by using FORMOSAT-2 images," *Int. J. Remote Sens.*, vol. 28, pp. 3071–3091, 2007.

[86] M. Yang, Y. Yang, and S. Hsu, "Application of remotely sensed data to the assessment of terrain factors affecting the Tsao-Ling landslide," *Can. J. Remote Sens.*, vol. 30, pp. 593–603, 2004.

[87] M. Yang, J. Lin, C. Yao, J. Chen, T. Su, and C. Jan, "Landslide-induced levee failure by high concentrated sediment flow—A case of Shan-An levee at Chenyulan River, Taiwan," *Eng. Geol.*, vol. 123, pp. 91–99, 2011.

[88] T. Lee and H. Yeh, "Applying remote sensing techniques to monitor shifting wetland vegetation: A case study of Danshui River estuary mangrove communities, Taiwan," *Ecol. Eng.*, vol. 35, pp. 487–496, 2009.

[89] G. Liu, T. Lin, and T. Kuo, "Estimation of Taiwan's Forested Areas by Classified NDVI Maps from NOAA AVHRR Data," *ISPRS J. Photogramm. Remote Sens.*, vol. 7, pp. 69–76, 2002.

[90] H. Wang and C. Huang, "Retrieving multi-scale climatic variations from high dimensional time-series MODIS green vegetation cover in a tropical/subtropical mountainous island," *J. Mt. Sci.*, vol. 11, pp. 407–420, 2014.

[91] C. Koh, P. Lee, and R. Lin, "Bird species richness patterns of northern Taiwan: Primary productivity, human population density, and habitat heterogeneity," *Divers. Distrib.*, vol. 12, pp. 546–554, 2006.

[92] P. Lee, T. Ding, F. Hsu, and S. Geng, "Breeding bird species richness in Taiwan: Distribution on gradients of elevation, primary productivity and urbanization," *J. Biogeogr.*, vol. 31, pp. 307–314, 2004.

- [93] N. Pettorelli *et al.*, "The normalized difference vegetation index (NDVI): unforeseen successes in animal ecology," *Clim. Res.*, vol. 46, pp. 15–27, 2011.
- [94] J. Lin, M. Yang, B. Lin, and P. Lin, "Risk assessment of debris flows in Songhe Stream, Taiwan," *Eng. Geol.*, vol. 123, pp. 100–112, 2011.
- [95] Department of Statistics, Ministry of the Interior, "Population," Taipei, Taiwan, 2014.
- [96] H. Hsu and C. Chen, "Observed and projected climate change in Taiwan," *Meteorol. Atmos. Phys.*, vol. 79, pp. 87–104, 2002.
- [97] C. Chen and Y. Chen, "The rainfall characteristics of Taiwan," *Mon. Weather Rev.*, vol. 131, pp. 1323–1341, 2003.
- [98] M. Yen and T. Chen, "Seasonal variation of the rainfall over Taiwan," *Int. J. Climatol.*, vol. 20, pp. 803–809, 2000.
- [99] T. Chen, M. Yen, J. Hsieh, and R. W. Arritt, "Diurnal and seasonal variations of the rainfall measured by the automatic rainfall and meteorological telemetry system in Taiwan," *Bull. Amer. Meteorol. Soc.*, vol. 80, pp. 2299–2312, 1999.
- [100] C. Hong, M. Lee, H. Hsu, and J. Kuo, "Role of submonthly disturbance and 40–50 day ISO on the extreme rainfall event associated with Typhoon Morakot (2009) in southern Taiwan," *Geophys. Res. Lett.*, vol. 37, pp. 1–6, 2010, article id L08805.
- [101] C. Chen, Y. Chen, C. Liu, P. Lin, and W. Chen, "Statistics of heavy rainfall occurrences in Taiwan," *Wea. Forecasting*, vol. 22, pp. 981–1002, 2007.
- [102] P. Yu, T. Yang, and C. Wu, "Impact of climate change on water resources in southern Taiwan," *J. Hydrol.*, vol. 260, pp. 161–175, 2002.
- [103] Central Weather Bureau, "Introduction to Taiwan's weather," Taipei, Taiwan, 2014.
- [104] J. Chen, H. Chen, and J. Liu, "Coherent interdecadal variability of tropical cyclone rainfall and seasonal rainfall in Taiwan during October," *J. Clim.*, vol. 26, pp. 308–321, 2013.
- [105] S. Wang, H. Cheng, and Y. Chao, "Natural seasons of the weather in the Taiwan area," *Atmos. Sci.*, vol. 11, pp. 101–120, 1984.
- [106] F. Zeng, G. J. Collatz, J. E. Pinzon, and A. Ivanoff, "Evaluating and quantifying the climate-driven interannual variability in global inventory modeling and mapping studies (GIMMS) normalized difference vegetation index (NDVI3g) at global scales," *Remote Sens.*, vol. 5, pp. 3918–3950, 2013.
- [107] E. Vermote and Y. Kaufman, "Absolute calibration of AVHRR visible and near-infrared channels using ocean and cloud views," *Int. J. Remote Sens.*, vol. 16, pp. 2317–2340, 1995.
- [108] J. Pinzon, M. E. Brown, and C. J. Tucker, "EMD correction of orbital drift artifacts in satellite data stream," in *Hilbert-Huang Transform and its Applications*, 2005, pp. 167–186.
- [109] J. E. Pinzon and C. J. Tucker, "A non-stationary 1981–2012 AVHRR NDVI3g time series," *Remote Sens.*, vol. 6, pp. 6929–6960, 2014.
- [110] B. N. Holben, "Characteristics of maximum-value composite images from temporal AVHRR data," *Int. J. Remote Sens.*, vol. 7, pp. 1417–1434, 1986.
- [111] J. Bi, L. Xu, A. Samanta, Z. Zhu, and R. Myneni, "Divergent arctic-boreal vegetation changes between North America and Eurasia over the past 30 years," *Remote Sens.*, vol. 5, pp. 2093–2112, 2013.
- [112] D. F. Watson, *Contouring: A Guide to the Analysis and Display of Spatial Data*. New York, NY, USA: Pergamon Press, 1992.
- [113] G. Pickup and B. Foran, "The use of spectral and spatial variability to monitor cover change on inert landscapes," *Remote Sens. Environ.*, vol. 23, pp. 351–363, 1987.
- [114] T. Su, M. Yang, T. Wu, and J. Lin, "Morphological segmentation based on edge detection for sewer pipe defects on CCTV images," *Expert Syst. Appl.*, vol. 38, pp. 13094–13114, 2011.
- [115] M. Yang and T. Su, "Segmenting ideal morphologies of sewer pipe defects on CCTV images for automated diagnosis," *Expert Syst. Appl.*, vol. 36, pp. 3562–3573, 2009.
- [116] R. A. Washington-Allen, R. D. Ramsey, T. G. Van Niel, and N. E. West, "Detection of harbingers of catastrophic regime shifts in drylands," in *Application of Threshold Concepts in Natural Resource Decision Making*. New York, NY, USA: Springer, 2014, pp. 273–289.
- [117] R. A. Washington-Allen, R. Ramsey, N. E. West, and B. E. Norton, "Quantification of the ecological resilience of drylands using digital remote sensing," *Ecol. Soc.*, vol. 13, pp. 33, 2008.
- [118] R. A. Washington-Allen, N. West, and R. D. Ramsey, "Remote sensing-based dynamical systems analysis of sagebrush steppe vegetation in rangelands," in *Proc. 7th Int. Rangelands Congr.*, 2003, pp. 416–418.
- [119] N. E. Zimmermann *et al.*, "Modern remote sensing for environmental monitoring of landscape states and trajectories," in *A Changing World*, New York, NY, USA: Springer, 2007, pp. 65–91.
- [120] P. Waylen, J. Southworth, C. Gibbes, and H. Tsai, "Time series analysis of land cover change: Developing statistical tools to determine significance of land cover changes in persistence analyses," *Remote Sens.*, vol. 6, pp. 4473–4497, 2014.
- [121] H. P. Tsai, J. Southworth, and P. Waylen, "Spatial persistence and temporal patterns in vegetation cover across Florida, 1982–2006," *Phys. Geogr.*, vol. 35, pp. 151–180, 2014.
- [122] M. Forkel, N. Carvalhais, J. Verbesselt, M. D. Mahecha, C. S. Neigh, and M. Reichstein, "Trend change detection in NDVI time series: Effects of inter-annual variability and methodology," *Remote Sens.*, vol. 5, pp. 2113–2144, 2013.
- [123] L. Eklundh, "Estimating relations between AVHRR NDVI and rainfall in East Africa at 10-day and monthly time scales," *Int. J. Remote Sens.*, vol. 19, pp. 563–570, 1998.
- [124] B. Li, S. Tao, and R. Dawson, "Relations between AVHRR NDVI and ecoclimatic parameters in China," *Int. J. Remote Sens.*, vol. 23, pp. 989–999, 2002.
- [125] S. Lu, J. D. Cheng, and K. N. Brooks, "Managing forests for watershed protection in Taiwan," *For. Ecol. Manage.*, vol. 143, pp. 77–85, 2001.
- [126] H. Chen and D. Petley, "The impact of landslides and debris flows triggered by Typhoon Mindulle in Taiwan," *Quart. J. Eng. Geol. Hydrogeol.*, vol. 38, pp. 301–304, 2005.
- [127] W. Teng, M. Hsu, C. Wu, and A. S. Chen, "Impact of flood disasters on Taiwan in the last quarter century," *Nat. Hazards*, vol. 37, pp. 191–207, 2006.
- [128] G. B. Crosta, "Introduction to the special issue on rainfall-triggered landslides and debris flows," *Eng. Geol.*, vol. 73, pp. 191–192, 2004.
- [129] D. K. Keefer, "Landslides caused by earthquakes," *Geol. Soc. Amer. Bull.*, vol. 95, pp. 406–421, 1984.
- [130] R. L. Schuster, A. S. Nieto-Thomas, T. D. O'Rourke, E. Crespo, and G. Plaza-Nieto, "Mass wasting triggered by the 5 March 1987 Ecuador earthquakes," *Eng. Geol.*, vol. 42, pp. 1–23, 1996.
- [131] S. J. Dadson *et al.*, "Earthquake-triggered increase in sediment delivery from an active mountain belt," *Geology*, vol. 32, pp. 733–736, 2004.
- [132] H. Hsu, C. Chou, Y. Wu, M. Lu, C. Chen, and Y. Chen, "Climate change in Taiwan: Scientific report 2011," National Science Council, Taipei, Taiwan, ROC, 2011, p. 67.
- [133] S. Self, J. Zhao, R. E. Holasek, R. C. Torres, and A. J. King, *The Atmospheric Impact of the 1991 Mount Pinatubo Eruption*. National Aeronautics and Space Administration, Washington, DC, USA, 1993.
- [134] S. Self, "The effects and consequences of very large explosive volcanic eruptions," *Philos. Trans. A Math. Phys. Eng. Sci.*, vol. 364, pp. 2073–2097, Aug. 15, 2006.
- [135] Y. Julien, J. A. Sobrino, and W. Verhoef, "Changes in land surface temperatures and NDVI values over Europe between 1982 and 1999," *Remote Sens. Environ.*, vol. 103, pp. 43–55, 2006.
- [136] S. Piao *et al.*, "Variation in a satellite-based vegetation index in relation to climate in China," *J. Veg. Sci.*, vol. 15, pp. 219–226, 2004.
- [137] C. J. Tucker, D. A. Slayback, J. E. Pinzon, S. O. Los, R. B. Myneni, and M. G. Taylor, "Higher northern latitude normalized difference vegetation index and growing season trends from 1982 to 1999," *Int. J. Biometeorol.*, vol. 45, pp. 184–190, 2001.
- [138] J. Hansen, R. Ruedy, M. Sato, and R. Reynolds, "Global surface air temperature in 1995: Return to pre-Pinatubo level," *Geophys. Res. Lett.*, vol. 23, pp. 1665–1668, 1996.
- [139] Y. Chiueh, C. Huang, and C. Tan, "Modeling the rice-climate indices in Taiwan," *Clim. Change Econ.*, vol. 4, no. 3, pp. 1–19, 2013, article id 1350012.
- [140] S. C. Liu, C. Wang, C. Shiu, H. Chang, C. Hsiao, and S. Liaw, "Reduction in sunshine duration over Taiwan: Causes and implications," *Terr. Atmos. Ocean Sci.*, vol. 13, pp. 523–546, 2002.
- [141] P. P. Wong *et al.*, "Climate change 2014: Impacts, adaptation, and vulnerability, part A: Global and sectoral aspects. contribution of working group II to the fifth assessment report of the intergovernmental panel on climate change," United Kingdom and New York, NY, USA, 2014, pp. 361–409.
- [142] IPCC, "Summary for policymakers," in *Managing the Risks of Extreme Events and Disasters to Advance Climate Change Adaptation*. C. B. Field *et al.*, Eds., A Special Report of Working Groups I and II of the Intergovernmental Panel on Climate Change. Cambridge, U.K. and New York, NY, USA: Cambridge University Press, 2012, pp. 1–19.
- [143] M. Lu, Y. Cho, S. Lee, C. Lee, and Y. Lin, "Climate variations in Taiwan during 1911–2009," *Atmos. Sci.*, vol. 40, pp. 297–321, 2012.
- [144] C. Shiu, S. C. Liu, and J. Chen, "Diurnally asymmetric trends of temperature, humidity, and precipitation in Taiwan," *J. Clim.*, vol. 22, pp. 5635–5649, 2009.

[145] S. C. Liu, C. Fu, C. Shiu, J. Chen, and F. Wu, "Temperature dependence of global precipitation extremes," *Geophys. Res. Lett.*, vol. 36, no. 17, pp. 1–4, 2009, article id L17702.

[146] J. Tu, C. Chou, and P. Chu, "The abrupt shift of typhoon activity in the vicinity of Taiwan and its association with western North Pacific-East Asian climate change," *J. Clim.*, vol. 22, pp. 3617–3628, 2009.

[147] J. Chen and H. Chen, "Interdecadal variability of summer rainfall in Taiwan associated with tropical cyclones and monsoon," *J. Clim.*, vol. 24, pp. 5786–5798, 2011.

[148] P. Chu, D. Chen, and P. Lin, "Trends in precipitation extremes during the typhoon season in Taiwan over the last 60 years," *Atmos. Sci. Lett.*, vol. 15, pp. 37–43, 2014.

[149] S. Piao *et al.*, "Interannual variations of monthly and seasonal normalized difference vegetation index (NDVI) in China from 1982 to 1999," *J. Geophys. Res. Atmos. (1984–2012)*, vol. 108, no. D14, pp. 1–13, 2003, article id 4401.

[150] P. Yu, T. Yang, and C. Kuo, "Evaluating long-term trends in annual and seasonal precipitation in Taiwan," *Water Resour. Manage.*, vol. 20, pp. 1007–1023, 2006.

[151] C. Hung, H. Hsu, and M. Lu, "Decadal oscillation of spring rain in northern Taiwan," *Geophys. Res. Lett.*, vol. 31, no. 22, pp. 1–4, 2004, article id L22206.

[152] M. A. Karori, J. Li, and F. Jin, "The asymmetric influence of the two types of El Niño and La Niña on summer rainfall over Southeast China," *J. Clim.*, vol. 26, pp. 4567–4582, 2013.

[153] M. Lu, C. Chen, and Y. Lin, "Long-term variation of the occurrence frequency of extreme rainfall events during the period of 1951–2005," *Atmos. Sci.*, vol. 35, pp. 87–103, 2007.

[154] C. Hung and P. Kao, "Weakening of the winter monsoon and abrupt increase of winter rainfalls over northern Taiwan and southern China in the early 1980s," *J. Clim.*, vol. 23, pp. 2357–2367, 2010.

[155] R. Fensholt and K. Rasmussen, "Analysis of trends in the Sahelian 'rain-use efficiency' using GIMMS NDVI, RFE, and GPCP rainfall data," *Remote Sens. Environ.*, vol. 115, pp. 438–451, 2011.

[156] Y. Richard *et al.*, "Interannual memory effects for spring NDVI in semi-arid South Africa," *Geophys. Res. Lett.*, vol. 35, no. 13, pp. 1–6, 2008, article id L13704.

[157] R. Aerts *et al.*, "Surface runoff and seed trapping efficiency of shrubs in a regenerating semiarid woodland in northern Ethiopia," *Catena*, vol. 65, pp. 61–70, 2006.

[158] X. Chuai, X. Huang, W. Wang, and G. Bao, "NDVI, temperature and precipitation changes and their relationships with different vegetation types during 1998–2007 in inner Mongolia, China," *Int. J. Climatol.*, vol. 33, pp. 1696–1706, 2013.

[159] N. G. McDowell *et al.*, "Global satellite monitoring of climate-induced vegetation disturbances," *Trends Plant Sci.*, vol. 20, no. 2, pp. 114–123, 2015.

[160] C. Chou, J. C. Chiang, C. Lan, C. Chung, Y. Liao, and C. Lee, "Increase in the range between wet and dry season precipitation," *Nat. Geosci.*, vol. 6, pp. 263–267, 2013.

[161] Y. Cho and M. Lu, "An analysis of the extreme dry spells in Taiwan and its variations during the recent one hundred years," *Atmos. Sci.*, vol. 41, pp. 171–187, 2013.

[162] Y. Bayarjargal, A. Karnieli, M. Bayasgalan, S. Khudulmur, C. Gandush, and C. Tucker, "A comparative study of NOAA–AVHRR derived drought indices using change vector analysis," *Remote Sens. Environ.*, vol. 105, pp. 9–22, 2006.

[163] Y. Lin, H. Chu, Y. Huang, C. Tang, and S. Rouhani, "Monitoring and identification of spatiotemporal landscape changes in multiple remote sensing images by using a stratified conditional Latin hypercube sampling approach and geostatistical simulation," *Environ. Monit. Assess.*, vol. 177, pp. 353–373, 2011.

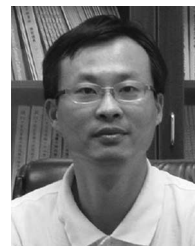
[164] H. Chen, M. Yang, C. Tang, and S. Wang, "Producing synthetic lightweight aggregates from reservoir sediments," *Constr. Build. Mater.*, vol. 28, pp. 387–394, 2012.



**Hui Ping Tsai** received the M.S. degree in bio-environmental systems engineering from the National Taiwan University, Taipei, Taiwan, in 2004, and the Ph.D. degree in geography from the University of Florida, Gainesville, FL, USA, in 2012.

Currently, she is a Postdoctoral Fellow with the Center for Environmental Restoration and Disaster Reduction, National Chung Hsing University, Taichung, Taiwan. Her research interests include remote sensing, land use and land cover change (LULCC), climate variability, and interaction

between human and environment.



**Ming-Der Yang** received the B.S. degree in civil engineering from the National Chiao Tung University, Hsinchu, Taiwan, in 1990, and the M.S. and Ph.D. degrees from the Department of Civil and Environmental Engineering and Geodetic Science, Ohio State University, Columbus, OH, USA, in 1993 and 1996, respectively.

Currently, he is a Professor with the Department of Civil Engineering, National Chung Hsing University. Many results about disaster investigation have been published by him on international journals. Recently,

research efforts have been put on developing 3-D reconstruction technology on remote sensing images for disaster monitoring and assessment. His research interests include image processing, remote sensing, geographic information system, environmental monitoring, and disaster assessment.